

Final Report

# Failure Analysis of Leak in Well Line from Aliso Canyon Natural Gas Storage Field

Southern California Gas  
Los Angeles, California

Report No.: OAPUS308RRICK (PP164597)  
November 8, 2016



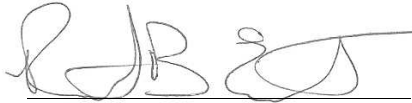
Southern California Gas  
 Failure Analysis of Leak in Well Line from Aliso Canyon Natural Gas Storage Field

Project Name:	Failure Analysis of Leak in Well Line from Aliso Canyon Natural Gas Storage Field	DET NORSKE VERITAS (U.S.A.), INC. (DNV GL) Oil & Gas Materials & Corrosion Technology Center Incident Investigation 5777 Frantz Road Dublin, OH 43017-1886 United States Tel: (614) 761-1214 Fax: (614) 761-1633 www.dnvgl.com
Customer:	Southern California Gas	
Contact Person:	Gerardo Zuniga	
Date of Issue:	November 08, 2016	
Project No.:	PP164597	
Organization Unit:	Incident Investigation	
Report No.:	OAPUS308RRICK	

Task and Objective:

Please see Executive Summary.

Prepared by



Richard B. Eckert  
Senior Principal Engineer

Verified by



John A. Beavers, Ph.D., FNACE  
Senior Principal Engineer

Approved by



David M. Norfleet, Ph.D., P.E.  
Head of Section –  
Incident Investigation

- Unrestricted Distribution (internal and external)
- Unrestricted Distribution within DNV GL
- Limited Distribution within DNV GL after 3 years
- No Distribution (confidential)
- Secret

Keywords

Copyright © DNV GL 2016. All rights reserved.

Rev. No.	Date	Reason for Issue:	Prepared by:	Verified by:	Approved by:
0	2016-11-08	First Issue			
1	2016-11-09	Final			

## Executive Summary

Southern California Gas (SoCal) retained Det Norske Veritas (U.S.A.), Inc. (DNV GL) to perform a metallurgical analysis on an above-grade section of pipe removed from the Ward 3A well withdrawal line that experienced a pinhole leak at the SoCal Aliso Canyon Natural Gas Storage Field. The leak was reported at 4:50 pm (PST) on 9/12/2016. The objective of the laboratory analysis was to determine the likely metallurgical causes(s) of the pinhole leak. DNV GL also provided field support and collected samples during the cut out of the pipe sample containing the pinhole leak.

SoCal provided DNV GL with a 3-foot long pipe cut-out, containing the well line leak, for analysis. Additionally, liquid, solid, and surface swab samples were collected by DNV GL personnel when the pipe sample was removed. The collected samples were analyzed as a part of this failure analysis.

***The leak resulted from localized corrosion at a single, isolated pit. The physical, metallurgical, chemical, and microbiological evidence do not convincingly support a particular corrosion mechanism, largely due to the conditions at the time of the cut out being dictated by the chemical batch treatment that had been applied in June 2016.***

Additional information pertaining to the history of operating conditions, internal corrosion monitoring, and inspection and mitigation specific to Ward 3A well line, should be reviewed to better correlate the results of this failure analysis with potential corrosion mechanisms.

The internal pit that caused the leak was isolated; nearly no other internal corrosion is present on the pipe sample. Although there was no evidence of a preexisting metallurgical defect or anomaly at the leak location, the morphology and appearance of the pit is unusual and thus, a metallurgical defect or anomaly that corroded out cannot be excluded as a cause of the leak.

Below is a summary of additional observations:

- The leak resulted from localized corrosion at a single, isolated pit.
- There was no evidence of significant general corrosion or pitting on the internal surface of the pipe, other than the pit that caused the leak.
- There was no evidence of general corrosion or pitting on the external surface of the pipe sample.

- The physical appearance and cross-sectional profile of the pit was somewhat unusual in that it exhibited angular features on the internal surface that are not typical of corrosion pits, and the profile had two distinct zones with different morphologies.
- Metallography did not indicate the presence of a mill defect, such as a scab or roll-in, that could have aided in the initiation of the isolated pit.
- The results of elemental analyses performed on internal deposits removed from the pipe sample identified high concentrations of potassium and chlorine; likely from the KCl water used in the batch treatment. Sulfur was present at 1.1% in Solid #1.
- EDS determined that the deposits present on the walls of the pit were primarily iron and oxygen, with minor levels of chlorine and trace levels of sulfur.
- XRD identified the crystalline compounds goethite-FeO(OH), sylvite-KCl, siderite-FeCO<sub>3</sub>, magnetite-Fe<sub>3</sub>O<sub>4</sub>, quartz-SiO<sub>2</sub> and lepidocrocite-FeO(OH) in sample Solid #1.
- The results of liquid composition analysis showed potassium and chloride to be the most abundant chemical species (likely from KCl water batch treatment). The pH of the liquid was between 7-8 as measured in the field.
- Residual glutaraldehyde (30 mg/L) was measured in the liquid sample. Viable bacteria numbers were very low in the liquid and fairly high in the surface samples.
- The results of bacteria culture testing provided no evidence that specific bacteria were preferentially flourishing at the pit location; there was no difference in the results from pit vs. uncorroded areas.
- The qPCR results identified significant numbers of bacteria in the well line that are common to soil and water, and that require oxygen for cell activity. These bacteria are not common to gas pipeline environments and may be more representative of contamination in the water used to make the batch treatment.
- Optical microscopy performed on three different surface swab samples collected from the internal surface of the pipe sample showed concentrations of cells that are consistent with the concentrations of bacteria measured using liquid culture media.
- No anomalies or linear indications were found on the OD surface of the pipe near the ERW weld seam using MPI.
- The microstructure of the pipe steel is consistent with the vintage and grade.
- The tensile properties of the base metal and weld seam meet the requirements for API 5LX Grade X42 line pipe steel in place at the time of construction.
- The chemical composition of the pipe sample meets requirements for API 5LX Grade X42 line pipe steel at the time of construction.

## Table of Contents

1.0	BACKGROUND .....	1
2.0	TECHNICAL APPROACH .....	1
3.0	RESULTS.....	4
3.1	Field Observations and Sampling.....	4
3.2	Visual Examination .....	4
3.3	Dimensional Analysis .....	5
3.4	Nondestructive Testing .....	5
3.5	Chemical Composition Testing .....	6
3.5.1	pH Testing.....	6
3.5.2	Qualitative Spot Testing .....	6
3.5.3	Energy Dispersive Spectroscopy of Deposits .....	6
3.5.4	X-Ray Diffraction Analysis .....	7
3.5.5	Chemical Composition of Liquid Sample .....	8
3.6	Microbiological Analysis.....	8
3.6.1	Serial Dilution Testing .....	8
3.6.2	Microscopic Examination for Total Bacteria .....	9
3.6.3	Molecular Microbiological Analysis .....	9
3.7	Metallographic Analysis and EDS .....	10
3.8	Mechanical Testing .....	11
3.9	Chemical Analysis of Pipe .....	12
4.0	CORROSION MECHANISM DISCUSSION .....	12
4.1.1	Operating Conditions .....	12
4.1.2	Internal Corrosion Mechanisms .....	14
4.1.2.1	H <sub>2</sub> S Corrosion .....	14
4.1.2.2	O <sub>2</sub> Corrosion .....	15
4.1.2.3	CO <sub>2</sub> Corrosion .....	15
4.1.2.4	Microorganisms.....	15
5.0	SUMMARY AND CONCLUSIONS .....	16

## Appendices

Appendix A – Summary of Genetic Microbiological Analysis, Liquid #1 and Solid #1 Samples

## List of Tables

Table 1.	Summary of liquid, solid, and swab samples collected from the internal surface of the pipe sample.....	19
Table 2.	Results of circumference and diameter measurements performed on the U/S and D/S ends of the pipe sample. ....	20
Table 3.	Results of wall thickness measurements performed on the U/S and D/S ends of the pipe sample.....	20
Table 4.	Results of spot tests performed on internal deposits on the pipe sample.....	20
Table 5.	Results of elemental analyses, using EDS, performed on Solid #1; internal deposits removed from the pipe sample. ....	21
Table 6.	Composition analysis results for sample Liquid #1.....	21
Table 7.	Results of bacteria culture testing performed on Liquid #1 and Swab Samples A, B and C, collected over a ~1 cm <sup>2</sup> area from the internal surface of the pipe sample. ....	22
Table 8.	Results of optical microscopy examination of Liquid #1 and Swab Samples A, B and C, collected over a ~1 cm <sup>2</sup> area from the internal surface of the pipe sample. ....	22
Table 9.	Results of bacteria DNA testing, using quantitative polymerase chain reaction, performed on Liquid #1 and Solid #1 samples.....	23
Table 10.	Results of tensile tests performed on transverse base metal and seam weld specimens removed from the pipe sample compared with requirements for API 5LX Grade X42 line pipe steel. ....	24
Table 11.	Results of Charpy V-notch impact tests performed on transverse base metal specimens removed from the pipe sample.....	24
Table 12.	Results of Charpy V-notch impact tests performed on centerline transverse seam weld specimens removed from the pipe sample. ....	25
Table 13.	Results of analyses of the Charpy V-notch impact energy and percent shear plots for transverse base metal and seam weld metal specimens removed from the pipe sample.....	25
Table 14.	Results of elemental analysis, using optical emission spectroscopy, performed on a base metal sample removed from the pipe sample.....	26
Table 15.	Five-Year Averages for Carbon Dioxide, Nitrogen, and Water Vapor at Four Aliso Canyon Gas Monitoring Locations.....	26

## List of Figures

Figure 1.	View of the well line looking west (downstream). Approximate axial location of the leak is indicated by the arrow. The pipeline is relatively horizontal here and the leak was at a slight sag or low spot.....	27
Figure 2.	View from a location just upstream of the leak, looking east (upstream). Well location is beyond the top of the hill.....	28
Figure 3.	Surface swabs, solid, and liquid samples collected by DNV GL personnel in the field when the pipe section was cut out. ....	29
Figure 4.	Photograph showing the as-received condition of the pipe sample; wrapped in plastic with the ends sealed. ....	30
Figure 5.	Photograph showing the pipe sample after unwrapping at the DNV GL lab. Flow direction and 12:00 position are marked on the pipe. Approximately half of the sample was used to machine specimens for mechanical testing. Location of leak (at 6:00) shown at arrow. ....	31
Figure 6.	Photograph showing a portion of the bottom half of the internal surface of pipe sample after it was split by cutting at the 3 and 9 orientation. The 6:00 orientation is shown by the dashed line and the leak/pit is shown at the arrow. Coloration of deposits on the internal surface illustrates historical liquid-level lines. ....	32
Figure 7.	Photograph showing the internal pipe surface at the leak/pit location after cleaning, dashed line shows the 6:00 orientation.....	33
Figure 8.	Photograph of the internal pipe surface at the leak/pit after cleaning.....	34
Figure 9.	XRD powder diffraction pattern of sample Solid #1.....	35
Figure 10.	Photograph showing the locations of three specimens removed for preparation of metallographic mounts from the pipe sample; M1 from the leak location, M2 from the ERW longitudinal seam and M3 from the pipe body. Dashed line shows orientation of ERM seam.....	36
Figure 11.	Photomicrograph of mount M1, showing the pit/leak (left) and the ERW weld seam (right). Areas that were analyzed using SEM/EDS are shown by the boxes labelled SEM 1 and SEM 2. Nital etch.....	37
Figure 12.	Photomicrograph of Mount M1 along the edge of the smooth, parabolic shaped zone of the pit cross section nearest the internal surface of the pipe. Magnification – 100X. Nital etch. (ID surface towards the top of photo; mirror image or area shown in Figure 11).....	38



## List of Figures (continued)

Figure 13.	Photomicrograph of Mount M1 along the edge of the narrow zone in the pit cross section showing significant undercutting. Magnification – 100X. Nital etch. (ID surface towards the top of photo; mirror image or area shown in Figure 11).	39
Figure 14.	SEM/EDS composite image showing distribution of iron (Fe) and oxygen (O) in the deposit layer on the pit surface in the smooth, parabolic zone, location SEM 1 in Figure 11. Original magnification – 200X.	40
Figure 15.	SEM/EDS composite image showing distribution of iron (Fe) and oxygen (O) in the scale layer on the pit surface near the leak at the OD surface, location SEM 2 in Figure 11; original magnification – 50X. (Image inverted from its actual position in service.)	41
Figure 16.	Photomicrograph of Mount M2 showing the centerline of the ERW seam weld (center of photo). Magnification – 100X. Nital etch.	42
Figure 17.	Photomicrograph of Mount M3 showing the microstructure of the pipe body away from the leak and away from the ERW weld. Magnification – 100X. Nital etch.	43
Figure 18.	Percent shear from Charpy V-notch tests as a function of temperature for transverse specimens removed from the base metal of the pipe sample.	44
Figure 19.	Charpy V-notch impact energy as a function of temperature for transverse specimens removed from the base metal of the pipe sample.	44
Figure 20.	Percent shear from CVN tests as a function of temperature for transverse specimens removed from the seam weld centerline of the pipe sample.	45
Figure 21.	CVN impact energy as a function of temperature for transverse specimens removed from the seam weld of the pipe sample.	45

## 1.0 BACKGROUND

Southern California Gas (SoCal) retained Det Norske Veritas (U.S.A.), Inc. (DNV GL) to perform a metallurgical analysis on an above-grade section of pipe removed from the Ward 3A well withdrawal line that experienced a pinhole leak at the SoCal Aliso Canyon Natural Gas Storage Field. The leak was reported at 4:50 pm (PST) on 9/12/2016. The objective of the laboratory analysis was to determine the likely metallurgical causes(s) of the pinhole leak. DNV GL also provided field support and collected samples during the cut out of the pipe sample containing the pinhole leak.

The pipe was reported to be 8-5/8-inch nominal outside diameter by 0.250-inch nominal wall thickness, API 5LX Grade X42, with an electric resistance welded (ERW) longitudinal seam. The well line name is "AGW569FB."

The well line was installed in 1982 and was externally coated/painted. The maximum allowable operating pressure (MAOP) of the line is 710 psig and the normal operating pressure was reported to be 500 to 550 psig. The operating pressure at the time the leak was discovered was 404 psig and the line was not flowing gas. The well line was reported to be last hydrostatically tested at 1,150 psig for 8 hours. The well line operates intermittently and had only 90 hours of operation (flow) in the last 10 years. A chemical batch treatment of corrosion inhibitor and biocide was applied to the well line on 6/22/2016.

SoCal provided DNV GL with a 3-foot long pipe cut-out, containing the well line leak, for analysis. Additionally, liquid, solid, and surface swab samples were collected by DNV GL personnel when the pipe sample was removed. The collected samples were analyzed as a part of this failure analysis.

## 2.0 TECHNICAL APPROACH

The procedures used in the analysis were in accordance with industry-accepted standards. Eight of the general standards governing terminology, bacteria testing, specific metallographic procedures, mechanical testing, and chemical analysis are as follows:

- NACE/ASTM G193 – 10a "Standard Terminology and Acronyms Relating to Corrosion."
- ASTM E7, "Standard Terminology Relating to Metallography."
- NACE TM0212, "Standard Test Method for Detection, Testing, and Evaluation of Microbiologically Influenced Corrosion on Internal Surfaces of Pipelines."
- NACE TM0194, "Standard Test Method for Field Monitoring of Bacterial Growth in Oil and Gas Systems."

- ASTM E3, "Standard Methods of Preparation of Metallographic Specimens."
- ASTM E8, "Test Methods for Tension Testing of Metallic Materials."
- ASTM E23, "Standard Test Methods for Notched Bar Impact Testing of Metallic Materials."
- ASTM A751, "Standard Test Methods, Practices, and Terminology for Chemical Analysis of Steel Products."

DNV personnel were present when the pipe sample was cut from the well line on 9/22/2016. At that time, DNV GL personnel collected the following samples:

- Liquid (Liquid #1) that drained out of the pipe when it was first cut (one Nalgene bottle ~500 mL and one smaller sample ~15 mL).
- Surface swabs (collected using sterile buffer solution to create a suspension) of the internal surfaces of the pipe at the leak location (6:00 orientation; Swab A), away from the leak at the 6:00 orientation (Swab B), and at the 12:00 orientation (Swab C).
- Solid residue that was present on the internal surface of the pipe along the 6:00 orientation (Solid #1).

Table 1 provides a summary of the samples collected and the chemical analyses that were performed. In the field, the pH of the liquid was measured and the solid residue was tested for the presence of sulfides and carbonates. The samples were stored in a cooler with cold packs, shipped with cold packs on 9/23/2016, and received on 9/24/2016 at the DNV GL laboratory in Dublin, Ohio. A portion of the solid residue sample and the smaller vial containing a portion of the liquid sample were shipped overnight, on cold packs, to a laboratory contracted by DNV GL for molecular microbiological analysis.

- The liquid sample was analyzed for metals, anions, residual glutaraldehyde and volatile fatty acids (VFA).
- A portion of the liquid sample and each of the swab sample suspensions were used to inoculate 6 types of liquid culture media to assess the numbers of viable bacteria. Liquid culture media for acid-producing bacteria (APB), sulfate-reducing bacteria (SRB), aerobic bacteria (AERO), anaerobic bacteria (ANA), iron-reducing bacteria (IRB), and nitrate-reducing bacteria (NRB) were used for the serial dilutions to evaluate growth of various types of bacteria. A five-vial serial dilution (1:10,000) was performed using each type of media for each collected sample.
- A 1 mL portion of the liquid sample and of each swab sample was fixed in 1% glutaraldehyde for epifluorescent microscopy. Five and ten microliter samples removed from the fixed samples were prepared for examination by drying on a

microscope slide and staining with 0.1% fluorescein isothiocyanate (FITC). The samples were examined using a CFI PLAN FLUOR 100X oil immersion objective on a Nikon Eclipse 50i epifluorescent microscope equipped with a FITC filter set to determine bacteria cell counts and morphology. The practical minimum detection limit for this method is approximately  $1 \times 10^3$  cells/ml of fixed sample.

- A portion of samples Liquid #1 and Solid #1 were subjected to quantitative polymerase chain reaction (qPCR) and processed to identify specific microorganisms and functional groups.

After the pipe sample was received at DNV GL on 9/26/2016, the following steps were performed for this analysis.

The pipe sample was visually examined and photographed in the as-received condition. The sample was removed from its packaging and photo documented. Circumferences, diameters, and wall thicknesses were then measured at the upstream (U/S) and downstream (D/S) ends of the pipe sample, where there was minimal corrosion.

Wet magnetic particle inspection (MPI), using the white contrast paint method, was used to inspect the longitudinal seam and three inches circumferentially on both sides of the seam on the OD surface of the pipe sample.

Compositional analyses performed on the internal deposits included: chemical spot testing on the pipe surface for carbonates and sulfides, elemental analyses using energy dispersive spectroscopy (EDS) with a scanning electron microscope (SEM), and compound analysis using X-ray diffraction (XRD).

Next, the pipe sample was split longitudinally along the 3:00 and 9:00 orientations to examine and photograph the internal surface. The orientations selected for splitting the pipe sample were chosen in order to preserve the internal corrosion features at the 6:00 orientation. The internal surface on the pipe sample was photo-documented. The deposits present on the internal surface of the pipe sample were then removed using Presolve®, and scotch bright pads. The internal surface was photographed again after cleaning.

One transverse cross-section was removed through the leak location (M1) and two other cross-sections were removed away from the leak location to examine the ERW seam weld (M2) and pipe body (M3) for metallographic analysis. The M1 cross-section was mounted, polished, and examined in the SEM, using EDS to produce elemental maps of deposits within the pit. The M1 cross section was then repolished, etched, and light photomicrographs were taken of all three mounted samples to document the microstructure of the pipe steel in the areas selected.

Duplicate tensile testing of the pipe body and seam weld (transverse specimens) and Charpy V-notch (CVN) impact testing (full curve) of the pipe body and seam weld center line were performed on samples removed from the pipe cut-out to document the mechanical properties.

Chemical analysis, using optical emission spectrometry (OES), was also performed on a steel sample removed from the pipe sample to determine the composition.

## 3.0 RESULTS

### 3.1 Field Observations and Sampling

Figure 1 and Figure 2 show the Ward 3A well line viewing to the west and to the east, respectively, from near the leak location. The pipeline is relatively horizontal near the leak location with a slight decline. The leak occurred at a slight sag or local low spot, at what appeared as a small pinhole at the 6:00 position, near the ERW seam weld. No external corrosion was noted on the outer surface of the pipe.

Figure 3 shows the samples that were collected by DNV GL personnel in the field when the pipe was first cut, and Table 1 provides a summary of the surface swab, liquid, and solid samples that were collected. An estimated 2-3 gallons of liquid drained from the pipe after it was cut.

### 3.2 Visual Examination

The pipe sample was documented in the condition in which it was received at DNV GL. Figure 4 shows the as-received condition of the pipe sample before unwrapping. The pipe was wrapped with plastic sheeting and the ends of the pipe were sealed with tape.

Figure 5 shows the pipe sample after unwrapping from the packaging. Field markings were present on the pipe and identified the flow direction and the 12:00 orientation. The pipe sample measured approximately 3 feet in length. The ERW weld seam was near the 6:00 orientation. No girth weld was present. The leak occurred at a pit on the internal surface located approximately 5 inches D/S from the U/S cut end. The leak/pit was not in the ERW seam but was located about 0.3 inches away circumferentially. No other visible pitting was observed before cleaning was performed on the internal surface. No evidence of general corrosion or pitting was observed on the external surface of the pipe. The external coating on the pipe was removed in the field before the pipe sample was cut out.

Figure 6 shows the internal surface of the bottom half of the pipe sample after it was split longitudinally and before it was cleaned. The coloration of the deposits on the internal

surface suggests the presence of historical liquid levels in the well line. No evidence of internal corrosion was noted on the top half of the pipe.

Figure 7 shows the leak location after cleaning the internal surface of the pipe sample. The surface texture of the pipe shows that the leak occurred in a smoother area or band along the bottom of the pipe (note: there was no wall loss in the band). Above the band, the pipe surface is more rough, with a hard, tenacious material on the surface that cannot easily be removed. Figure 8 shows a close up of the leak location after cleaning. The leak occurred at a pit approximately 0.4 inches long (axial) and 0.3 inches wide (circumferentially). The pit has an angular appearance at the pipe surface that is not typical of most corrosion. A few much smaller (<0.05 inches diameter and depth) pits were present in the smooth band along the bottom of the pipe; otherwise there was no other internal corrosion present.

### 3.3 Dimensional Analysis

Circumferences, diameters, and wall thicknesses were measured at the U/S and D/S ends of the pipe sample; see Table 2 for the results of the measurements. The diameters calculated from circumference measurements for the U/S and D/S ends were 8.656 inches and 8.675 inches, respectively. The calculated diameters meet the requirements in API 5LX for 8-inch diameter line pipe.<sup>1</sup> Diameter measurements were also determined using a tape measure from the 3:00 to 9:00 and 12:00 to 6:00 orientations to check for pipe ovality. All diameters for the pipe sample measured 8.63 inches, indicating no ovality.

Wall thicknesses were measured at the U/S and D/S ends of the pipe samples at the 12:00, 3:00, 6:00, and 9:00 orientations; see Table 3. The thickness measurements were taken in areas with minimal corrosion and no coating. The maximum, minimum, and average wall-thickness values for the pipe sample meet the requirements in API 5LX for line pipe with a nominal wall thickness of 0.250 inches.<sup>2</sup>

### 3.4 Nondestructive Testing

Wet MPI using the white contrast paint method was used to inspect the longitudinal seam and three inches circumferentially on both sides of the seam on the OD surface of the pipe sample. No cracks or linear indications were observed in the area that was inspected. The internal surface was not inspected to avoid contaminating the surface deposits.

---

1  $\pm 1\%$ , API 5LX Line Pipe Specifications, 23th Edition – March 1981.

2  $-12.5\%$ , API 5LX Line Pipe Specifications, 23<sup>th</sup> Edition, March 1981.

### 3.5 Chemical Composition Testing

One internal deposit sample, Solids #1, was collected in the field from the pipe sample for analysis. The results of the analyses performed on the internal deposits and deposits remaining on the pipe surface are discussed below individually.

#### 3.5.1 pH Testing

The pH on the internal pipe surface within the deposits was determined in the DNV GL laboratory using deionized (DI) water and pH test paper. The pH measurements were obtained by placing a few drops of deionized (DI) water on the pH test paper and then the wetted paper was placed in contact with the deposits on the pipe surface. The pH test paper was examined for color changes and compared to pH color charts. The pH of deposits on the pipe surface was measured to be 8.

The Solid #1 sample was not tested for pH to conserve the sample for other analyses.

#### 3.5.2 Qualitative Spot Testing

Qualitative spot testing, using 2N HCl, was performed on deposits (Solid #1) in the field and directly on the pipe sample at the DNV GL laboratory. In the lab test, a few drops of the HCl were placed on the deposits and a piece of lead acetate paper, which was wetted with deionized water, was held near the acid droplet on the surface. Vigorous bubbling is a positive indication for the presence of carbonates. A tan to brown color change for the lead acetate paper and/or a rotten egg odor are positive indications for the presence of sulfides. The deposits tested negative for the presence of carbonates and sulfides.

In the field, the collected solids were found to be relatively magnetic and were also tested for the presence of carbonates and sulfide. The field test did not produce detectable spot test indications of either carbonates or sulfides. Table 4 shows the results of the spot tests.

#### 3.5.3 Energy Dispersive Spectroscopy of Deposits

Table 5 shows the average of five EDS analyses performed on the internal deposits collected from the pipe sample (Solids #1). The results indicate that the sample was comprised of 44.5% iron (Fe), 19% carbon (C), and 29.2% oxygen (O). Other elements that were present in lesser amounts included 1.1% sulfur (S), 1.9% chlorine (Cl), 2% potassium (K), and 0.8% silicon (Si).

EDS of discrete particles in the solid sample was also performed at 500X. One particle was found to be 34% K and 31% Cl; likely remaining from evaporated KCl water; common in well-work fluids.

The sulfur that was detected can be present in several forms including sulfates, elemental sulfur, and sulfides (e.g., iron sulfide). Sulfates and sulfides can originate from the formation. Sulfates act as a terminal electron acceptor for SRB that produce sulfide. Sulfides also can form as a result of corrosion reactions between the pipe and H<sub>2</sub>S within the gas if any water is present.

Chlorides are known to promote localized corrosion of carbon steels by breaking down the passive layers on carbon steels in aqueous environments. Chlorides originate in produced water and in well work fluids, such as KCl water.

Iron is a primary element in steel. Oxygen is common in corrosion products such as oxides and carbonates, regardless of whether oxygen was present in the gas.

EDS was also performed on deposits that were present in the mounted cross sections of the pit; information on those samples is provided in along with metallography in Section 3.7.

#### 3.5.4 X-Ray Diffraction Analysis

Figure 9 shows the results of the XRD analyses performed on the internal deposits in Solid #1. XRD analysis of this material identified the crystalline compounds goethite-FeO(OH), sylvite-KCl, siderite-FeCO<sub>3</sub>, magnetite-Fe<sub>3</sub>O<sub>4</sub>, quartz-SiO<sub>2</sub> and lepidocrocite-FeO(OH). The results are not quantitative. No further XRD analysis was able to be performed as there were very few deposits that could be collected from the pipe surface or in the pit during the laboratory examination.

Magnetite is a common iron oxide associated with the corrosion of carbon steel that forms in relatively low oxygen conditions. Magnetite is also a predominant constituent of mill scale. Goethite is a hydrated ferric oxide that forms under oxidizing conditions at temperatures below 200 °C.

Siderite is an iron carbonate that can form in the presence of dissolved CO<sub>2</sub> within the transported product or may precipitate from oxygen corrosion in saturated waters.

Lepidocrocite can be a decomposition product of mackinawite, a form of iron sulfide that is attributed to SRB activity.

Quartz is found in sand and sylvite likely represents the dried residue of KCl water used in preparing the chemical treatment for the pipeline. See Section 4.1.1.



### 3.5.5 Chemical Composition of Liquid Sample

The field pH of the liquid sample was measured to be between 7 and 8 at the time of collection. Liquid #1 sample was analyzed for anions, cations, glutaraldehyde, and volatile fatty acids (VFA). Results of the liquid composition analysis are shown in Table 6.

For the Liquid #1 sample, potassium (20,300 mg/L) and chloride (17,700 mg/L) were the highest level components. Iron was measured to be 63.4 mg/L. Sulfate (131 mg/L) and nitrate (0.78 mg/L) were present, and both species can be used by certain bacteria for growth. All of the VFAs that were tested for were below the detection limit of 1.67 ppm. VFAs can be formed as metabolic products of microbial activity, particularly acid producing and fermentative bacteria.

On 9/26/2016, glutaraldehyde residual was measured on sample Liquid #1 using a Hach biocide test kit model GT-1 (Cat. No. 25872-00). The glutaraldehyde residual was measured to be 30 mg/L.

## 3.6 Microbiological Analysis

The results of the microbiological analyses are discussed below, individually.

### 3.6.1 Serial Dilution Testing

Table 7 shows the results of the bacteria serial dilution testing for Swabs A, B and C, and Liquid #1, collected from the pipe sample at the time of the cut out. A review of the collective results shows that culturable aerobic, acid producing, and nitrate reducing bacteria were present in the pipe. Aerobes were the most prevalent group of bacteria present; as high as 100,000 cells/cm<sup>2</sup> for Swab C (12:00 position, away from leak), which is unusual for a typically anaerobic environment in a natural gas line. The numbers of bacteria were considerably higher on the surface samples (swabs) than in the liquid sample, as would be expected. No anaerobic bacteria were detected. No iron reducing or sulfate reducing bacteria were detected in any of the samples tested; most of these microorganisms are strict anaerobes and cannot live in the presence of oxygen. Nitrate reducers, which are not common to natural gas operations, were present in concentrations as high as 1,000 cells/cm<sup>2</sup>. Note that 0.78 mg/L of nitrate was measured in the Liquid #1 sample; no nitrite was detected.

Culture testing provided no evidence that specific bacteria were preferentially flourishing at the internal corrosion pit/leak location; there was no significant difference in the results from pitted vs. uncorroded areas at the time the samples were collected.

### 3.6.2 Microscopic Examination for Total Bacteria

The results of microscopic analysis of the three surface swab samples and the Liquid #1 sample are provided in Table 8. No bacteria were observed in the Liquid #1 sample, and rod-shaped cells in clusters were detected for all three surface swab samples. The calculated concentration of cells for Swab A (leak) was  $>7.00 \times 10^4$  cells/cm<sup>2</sup>. Swab Samples B and C had  $>1.40 \times 10^5$  cells/cm<sup>2</sup> present. The observation of these numbers of cells in the surface swabs is consistent with the fact that elevated numbers of viable bacteria were also recovered from the surface swabs using liquid culture media and measured using qPCR. The absence of cells in the Liquid #1 sample is consistent with very low numbers detected using culture media and the presence of residual glutaraldehyde in the liquid.

This type of microscopic examination does not differentiate between living and non-living organisms.

### 3.6.3 Molecular Microbiological Analysis

Table 9 shows the results of the qPCR testing of the Liquid #1 and Solid #1 samples collected from the pipe during the cut out. A graphical representation of the microbial populations measured in each sample is also provided in Appendix A. The qPCR method measures DNA from cells that are living, inactive, and dead; thus the cell counts from qPCR are typically much higher than those from culture based methods.

The total numbers of bacteria present, based on qPCR, were  $1.70 \times 10^5$  cell/mL for Liquid #1 sample and  $1.37 \times 10^8$  cells/cm<sup>2</sup> for the Solid #1 sample. The difference between these samples is not unexpected as microorganisms are nearly always more abundant on surfaces in biofilms than in the bulk liquid phase.

The primary types or groups of microorganisms detected using qPCR were iron reducers, iron oxidizers and nitrogen fixing bacteria. No SRB, or acid producing, fermentative bacteria were detected. A particular genus of iron reducer, *Anaeromyxobacter*, was measured to be  $4.26 \times 10^3$  cells/mL for Liquid #1 sample and  $2.27 \times 10^5$  cells/cm<sup>2</sup> for Solid #1. *Anaeromyxobacter* are delta-Proteobacteria found in soil and freshwater sediments. They are capable of using, e.g., oxygen, nitrate, nitrite, and soluble and amorphous ferric iron as electron acceptors, and a variety of compounds, including acetate and hydrogen, as electron donors. Iron oxidizers and reducers are often found together in the same environment because they mutually benefit one another through an iron redox couple or cycle. Nitrogen fixing bacteria are common to soil; converting nitrogen to ammonium which can be assimilated by other organisms. Neither *Anaeromyxobacter* nor nitrogen fixing bacteria are common to gas pipeline environments. Their presence may have originated in the water that was used to make the batch treatment that was applied to the well line. See Section

4.1.1. The qPCR results are consistent with the culture-based results in terms of the dominant types of microorganisms that were measured.

It should be noted that qPCR typically indicates the presence of numerous types of microorganisms, however; it does not indicate which microorganisms are active, as this depends on the local environment and the presence of energy sources and electron acceptors used for metabolism.

### 3.7 Metallographic Analysis and EDS

Three transverse cross-sections were removed through representative areas of the pipe sample for the preparation of metallographic mounts and for analysis. The locations of the Mounts M1, M2, and M3 are shown in Figure 10. Mount M1 was taken through the pit/leak, Mount M2 was taken away from the pit in the ERW seam, and Mount M3 was taken away from the pit in the pipe body.

Figure 11 is a stereo light photomicrograph of the transverse cross section in Mount M1; it shows the two locations where EDS elemental mapping was performed within the pit and the location of the ERW weld relative to the pit. The pit has two distinct “zones” as it penetrated through the pipe from the internal surface. The first zone is a smooth, roughly parabolic shape that is located nearest to the internal surface of the pipe; see Figure 12. The depth of the parabolic zone of metal loss is about 25% of the overall thickness of the pipe. The second zone in the pit cross section extends through the pipe wall from about the center of the parabolic area and is much narrower in width. The narrow zone also has undercutting in the pit walls, as shown in Figure 13. Adherent surface deposits were present on the walls of the pit in both zones; however, the undercut areas in the narrow zone of the pit had more deposits present. The microstructure surrounding the pit showed no evidence of grain deformation or decarburization band that would be expected if the pit resulted from, or initiated from, a mill defect, e.g., a rolled-in slug. No evidence of wall loss or pitting was apparent at the external surface of the pipe.

The adherent deposits present along the wall of the pit in Mount M1 were analyzed using SEM/EDS. Figure 14 shows a SEM/EDS composite image depicting the distribution of iron (Fe) and oxygen (O) in the deposit layer on the pit surface in the parabolic zone, location SEM 1 in Figure 11. Figure 15 is a SEM/EDS composite image in area SEM 2, depicting the distribution of iron (Fe) and oxygen (O) in the scale layer on the pit surface in the narrow zone. In the examination of both areas, some isolated areas of sulfur were observed and chlorine tended to be present at the interface between the deposit and the pipe steel. No major difference in the deposit composition between the two zones was observed and no unusual foreign material was found in the pit.

The ERW seam weld also is evident in Figure 11, located about 0.3 inches circumferentially from the through wall pit. The microstructure is typical of a high frequency ERW weld. A transverse cross section through the ERW seam weld, away from the corroded area, in Mount M2, is shown in Figure 16. The microstructure of the seam weld at this location and in Mount M1 showed no defects or unusual microstructural characteristics.

Figure 17 is a light photomicrograph showing the typical base metal microstructure for the pipe steel, in Mount M3. The microstructure consists of ferrite (white areas) and pearlite (black areas). This microstructure is typical for the grade and vintage of pipe.

There was no evidence of metallurgical defects in the steel microstructure within the 3 mounts examined.

### 3.8 Mechanical Testing

The results of tensile testing performed on transverse base metal and seam weld specimens removed from the pipe sample are shown in Table 10 along with the specifications for API 5LX Grade X42 welded pipe. The average yield strength (YS), ultimate tensile strength (UTS), and elongation for the transverse specimens meet the API specifications for API 5LX Grade X42 welded line pipe steel in place at the time of manufacture.

Table 11 and Table 12 present the detailed results of Charpy impact testing performed on transverse base metal and ERW seam weld (notch at weld centerline) specimens, respectively. Figure 18 and Figure 19 show the Charpy percent shear and impact energy curves for the base metal, respectively. Figure 20 and Figure 21 show the Charpy percent shear and impact energy curves for the seam weld specimens, respectively. An analysis of the data indicates that the 85% fracture appearance transition temperature (FATT) for the base metal is 69°F and the upper shelf Charpy energy is 35.2 ft·lbs, full size. The FATT for the seam weld was 97°F and the upper shelf Charpy energy is 24 ft·lbs, full size. See Table 13.

The Charpy V-notch test results can be adjusted to determine the 85% fracture appearance transition temperature (FATT) that would be expected for full-scale pipe by applying temperature shifts to the data. This method (full-scale) adjusts the 85% FATT obtained from the Charpy tests to a predicted FATT from the Battelle Drop-Weight Tear Test (BDWTT). The predicted 85% FATT from the BDWTT test most closely represents the expected FATT for full-scale pipe wall material.<sup>3</sup> The full-scale brittle to ductile transition temperature for the pipe and weld specimens (based on a pipe wall thickness of 0.250

3 W. A. Maxey, J. F. Kiefner, R. J. Eiber, *Brittle Fracture Arrest in Gas Pipelines*, NG-18 Report No. 135, A.G.A. Catalog No. L51436, April 1983, Battelle Columbus Laboratories.

inches) are shown in Table 13. The pipe material is expected to exhibit ductile fracture behavior above the full-scale transition temperature.<sup>4</sup>

### 3.9 Chemical Analysis of Pipe

The results of the chemical analysis performed on a base metal sample removed from the pipe sample are shown in Table 14. The results show that the pipe meets the compositional requirements for API 5LX Grade X42 welded line pipe steel in place at the time of manufacture.

## 4.0 CORROSION MECHANISM DISCUSSION

### 4.1.1 Operating Conditions

The Ward 3A well withdrawal line in the Aliso Canyon natural gas storage field operates at a normal pressure 500-550 psig. The normal operating temperature was not reported. The well line experiences unidirectional flow with only intermittent use; once a year was reported. The well line experienced just 90 hours of operation (flow) in the last 10 years. The flow rates during operation were not reported. The well line is not a dead leg by design. The pin hole leak that was discovered was not near a tie-in point, injection quill, facility, appurtenance, etc. The leak was 7 feet from an U/S girth weld and 5.6 feet from a D/S girth weld, at a local low point in elevation profile.

Some gas composition data were reviewed for the storage field, overall, although not specifically for the well line that leaked. Table 15 presents the average CO<sub>2</sub>, nitrogen, and water vapor values at four Aliso Canyon gas monitoring locations over the past five years. The highest average CO<sub>2</sub> value for the past 5 years was 1.08 mol%, resulting in a low partial pressure of 5.94 psig CO<sub>2</sub> at 550 psig. Nitrogen levels, which can be used to indicate possible air (and oxygen) in the gas stream, have been very low. Water vapor levels in the gas being monitored at two SoCal dehydration units were reviewed. In general, much of the gas is wet or water saturated upon withdrawal, which is not unusual for gas storage fields. The five year average water vapor level for one dehydration unit inlet was 28.23 lbs/Mscf. Water saturation and condensation is dependent upon water vapor content of the gas, temperature and pressure.

Historical internal corrosion monitoring or inspection data were not reviewed on the well line as a part of this failure analysis. SoCal reported that there were no previous leaks on the well line.

---

4 Rosenfeld, M.J., "A Simple Procedure for Synthesizing Charpy Impact Energy Transition Curves from Limited Test Data," International Pipeline Conference, Volume 1, ASME, 1996, Equation 1.

SoCal reported that, on 6/22/2016, 71 barrels of chemical batch treatment were injected into the Ward 3A well line for corrosion protection while the line was not flowing. The batch treatment was made up using several different chemical products and dosages before it was injected, as listed below:

**X-Chem CW 1622:** Corrosion inhibitor, 500 ppm

Methyl alcohol, Benzyl alkyl pyridinal quaternary ammonium chloride, fatty acids, Coco alkyl dimethyl benzyl ammonium chloride, ethanol 2-2-oxybis reaction products with ammonia, hydrochloric acid, isopropyl alcohol

**X-Chem CW 1630:** Corrosion inhibitor, 250 ppm

(n-Alkyl (C12-C16) dimethyl benzyl ammonium chloride) and isopropyl alcohol

**Aqua Car 742:** Biocide, 500 ppm

Glutaraldehyde 42.5%, quaternary ammonium compounds 7.5%, ethanol <1%, methanol <=0.42%, water <=48.6%

**C-166:** Oxygen scavenger, 120 ppm

Ammonium bisulfite, proprietary phosphonate, ammonium chloride, methyl alcohol, DETA phosphonate ammonium salt

**Water (3% KCl):** Balance (carrier)

Potassium chloride mixture (common for well work) and fire water at Aliso Canyon may have also been used.

The majority of the chemical batch was KCl water (concentration unknown). The details of how the batch was prepared; the water sources used and water quality, and method of delivery to the pipeline, were not reviewed. Glutaraldehyde is known to be deactivated by ammonium and sodium bisulfite, and by primary amines. The water sample recovered from the pipe was high in potassium and chloride, and contained 30 mg/L glutaraldehyde; thus it appeared to be at least, in part, from the batch treatment applied in June 2016. As discussed previously, significant levels of viable aerobic bacteria were recovered from surface swabs, indicating that the batch treatment had not killed all bacteria living on the surface of the pipe.

The internal corrosion mitigation and monitoring history of the well line were not reviewed as a part of this failure analysis. It is not known as to whether the well line is piggable.

#### 4.1.2 Internal Corrosion Mechanisms

There are four primary causes of internal pitting failures in pipelines and three are associated with dissolved gas related mechanisms: hydrogen sulfide (H<sub>2</sub>S), carbon dioxide (CO<sub>2</sub>), and oxygen (O<sub>2</sub>). The fourth mechanism is microbiologically influenced corrosion (MIC); caused by the presence and/or activity of microorganisms on the steel surface. All of these mechanisms require the presence of water for corrosion to occur, and were considered in this investigation.

The pipe that leaked was located in a local low spot relative to the immediate elevation profile, where water could collect. Historical liquid level lines were observed in the well line at the cut-out location. The well line was seldom used; thus, any water produced with the gas during withdrawal, or any condensed water, would remain in the well line when it was not flowing. The observation of high numbers of bacteria at the 12:00 position on the pipe sample suggests that either water was condensing on the top half of the pipe or the pipe was full of water at this location.

The corrosion damage that caused the leak was a single isolated pit, located where there was nearly no other corrosion present. The presence of a solid deposit or occlusion on the pipe surface can sometimes result in the fixation of an anodic site, although no such deposit was found in the well line. The physical appearance and cross sectional profile of the pit was somewhat unusual in that it exhibited angular features on the internal surface that are not typical of corrosion pits, and the profile had two distinct zones with different morphologies. Metallography did not indicate the presence of a mill defect, such as a scab or roll-in, which could have aided in the initiation of the isolated pit. The two different zones in the pit cross section could have also represented two different periods of time where one corrosion mechanism was prevalent, followed by a different mechanism.

##### 4.1.2.1 H<sub>2</sub>S Corrosion

Whether or not hydrogen sulfide was present in the storage field and the concentration was not reported. In the presence of hydrogen sulfide, corrosion products typically contain sulfides (e.g., iron sulfide).

Sulfur (1.1%) was detected in sample Solid #1 using EDS; however, the spot tests and XRD results did not indicate that sulfides were present. Small amounts of sulfur were also detected in the EDS examination of the deposits on Mount M1, in the pit. One way lepidocrocite (identified by XRD in Solid #1) can form is as a primary decomposition product of mackinawite; an iron sulfide often associated with SRB activity. However, the origin of the lepidocrocite cannot be proven. No sulfate reducing bacteria or archaea (which produce sulfide) were found to be present in the swab samples or Solid #1. However, the effect of

the batch treatment on the conditions present when the pipe was cut and sampled need to be considered, as they may have been significantly different than the normal operating conditions.

#### 4.1.2.2 O<sub>2</sub> Corrosion

Transmission quality natural gas, such as that stored in Aliso Canyon field, is normally low in oxygen. Nitrogen levels reviewed for certain monitoring locations in the field over the last 5 years were low, suggesting that air was not being blended into the gas. Again, data specific to the well line Ward 3A were not reviewed.

XRD showed the presence of iron oxides in Solid #1 including goethite-FeO(OH), magnetite-Fe<sub>3</sub>O<sub>4</sub>, and lepidocrocite-FeO(OH). The origins of these oxides has been discussed previously. Goethite and lepidocrocite are commonly associated with corrosion of iron in the presence of oxygen.

In oxygen corrosion, it is more typical to observe corrosion on all water-wet surfaces; not a single isolated pit on a pipe surface that has little other corrosion. The volume of corrosion products was also minimal in the well line that leaked; whereas, oxygen commonly produces a large volume of corrosion products.

The results from bacteria culture testing demonstrated an abundance of viable *aerobic* microorganisms and no bacteria that were primarily anaerobic; however, this finding may not be relevant to the normal operating conditions in the well line because the aerobes could have been introduced with the batch treatment water.

#### 4.1.2.3 CO<sub>2</sub> Corrosion

Based on the information available, carbon dioxide was likely not the primary cause for the pitting, as more of the pipe surface would have been corroded. Carbonates were not detected in the spot tests, but siderite (FeCO<sub>3</sub>) was detected by XRD. Siderite forms in the presence of CO<sub>2</sub> and is typically the dominant corrosion product that is associated with CO<sub>2</sub> corrosion. The CO<sub>2</sub> levels in Aliso Canyon gas in general are low; however, the CO<sub>2</sub> level specific to the well line was not reported.

#### 4.1.2.4 Microorganisms

As discussed in the previous section, the effect of the batch treatment on the results of various tests performed in this failure analysis need to be considered; particularly in terms of microbiology. Considerations include:

- Culture testing provided no evidence that specific bacteria were preferentially flourishing at the internal corrosion pit/leak location; there was no significant



difference in the culture results from the pit/leak vs. uncorroded areas at the time the samples were collected.

- No anaerobic bacteria were detected, as would be expected in a pipeline that is typically anaerobic. No anaerobic iron reducing or sulfate reducing bacteria were detected in any of the samples tested.
- Nitrate reducing bacteria, which are not common to natural gas storage operations, were present in concentrations as high as 1,000 cells/cm<sup>2</sup>.
- Viable bacteria counts were elevated in Swab C at the 12:00 orientation in the pipe, and similar to the bacteria counts at the 6:00 position, suggesting that the entire internal surface of the pipe had been wet or had condensation present.
- Significant numbers of nitrogen fixing bacteria and *Anaeromyxobacter* were found using qPCR; these bacteria are common to soil and water and require some oxygen for cell activity. These bacteria are not common to gas pipeline environments.

Since the water in the well line at the time of the cut out appeared to be primarily from the batch treatment, it is possible that the nitrogen fixing bacteria and *Anaeromyxobacter* are indicative of contamination in the water used for batch treatment, rather than a routinely aerobic environment in the well line.

The microbiological data produced for this failure analysis do not clearly support any specific MIC mechanism, based on the limited operating information available.

## 5.0 SUMMARY AND CONCLUSIONS

The physical, metallurgical, chemical, and microbiological conditions that are evidenced by the results of this failure investigation do not convincingly support a particular corrosion mechanism, largely due to the conditions at the time of the cut out being dictated by the chemical batch treatment that had been applied in June 2016. Additional information pertaining to the history of operating conditions, internal corrosion monitoring, and inspection and mitigation specific to Ward 3A well line, should be reviewed to better correlate the results of this failure analysis with potential corrosion mechanisms.

The internal pit that caused the leak was isolated; nearly no other internal corrosion is present on the pipe sample. Although there was no evidence of a preexisting metallurgical defect or anomaly at the leak location, the morphology and appearance of the pit is unusual and thus, a metallurgical defect or anomaly that corroded out cannot be excluded as a cause of the leak.

Below is a summary of additional observations:

- The leak resulted from localized corrosion at a single, isolated pit.

- There was no evidence of significant general corrosion or pitting on the internal surface of the pipe, other than the pit that caused the leak.
- There was no evidence of general corrosion or pitting on the external surface of the pipe sample.
- The physical appearance and cross-sectional profile of the pit was somewhat unusual in that it exhibited angular features on the internal surface that are not typical of corrosion pits, and the profile had two distinct zones with different morphologies.
- Metallography did not indicate the presence of a mill defect, such as a scab or roll-in, that could have aided in the initiation of the isolated pit.
- The results of elemental analyses performed on internal deposits removed from the pipe sample identified high concentrations of potassium and chlorine; likely from the KCl water used in the batch treatment. Sulfur was present at 1.1% in Solid #1.
- EDS determined that the deposits present on the walls of the pit were primarily iron and oxygen, with minor levels of chlorine and trace levels of sulfur.
- XRD identified the crystalline compounds goethite-FeO(OH), sylvite-KCl, siderite-FeCO<sub>3</sub>, magnetite-Fe<sub>3</sub>O<sub>4</sub>, quartz-SiO<sub>2</sub> and lepidocrocite-FeO(OH) in sample Solid #1.
- The results of liquid composition analysis showed potassium and chloride to be the most abundant chemical species (likely from KCl water). The liquid sample also had sulfate (131 mg/L) and nitrate (0.78 mg/L) present; both species can be used by certain bacteria for growth. The pH of the liquid was between 7-8 as measured in the field.
- Residual glutaraldehyde (30 mg/L) was measured in the liquid sample. Viable bacteria numbers were low in the liquid and fairly high in the surface samples.
- The results of bacteria culture testing provided no evidence that specific bacteria were preferentially flourishing at the pit location; there was no difference in the results from pit vs. uncorroded areas.
- Significant numbers of nitrogen fixing bacteria and *Anaeromyxobacter* were found using qPCR; these bacteria are common to soil and water and require some oxygen for cell activity. These bacteria are not common to gas pipeline environments and may be more representative of contamination in the water used to make the batch treatment.
- Optical microscopy performed on three different surface swab samples collected from the internal surface of the pipe sample showed concentrations of cells that were consistent with the concentrations of bacteria measured using liquid culture media.
- No anomalies or linear indications were found on the OD surface of the pipe near the ERW weld seam using MPI.
- The microstructure of the pipe steel is consistent with the vintage and grade.

- The tensile properties of the base metal and weld seam meet the requirements for API 5LX Grade X42 line pipe steel in place at the time of construction.
- The chemical composition for the pipe sample meets requirements for API 5LX Grade X42 line pipe steel at the time of construction.

Table 1. Summary of liquid, solid, and swab samples collected from the internal surface of the pipe sample.

Sample Identification	Approximate Orientation	Analyses Performed									
		Spot Testing	EDS	XRD	pH	qPCR	Serial Dilution	Microscopic Exam	Glutaraldehyde Residual	Anions and Cations	Volatile Fatty Acids
Liquid #1	NA	-	-	√	√	√	√	√	√	√	√
Swab A	6:00 at leak	-	-	-	-	-	√	√	-	-	-
Swab B	6:00 away from leak	-	-	-	-	-	√	√	-	-	-
Swab C	12:00 away from leak	-	-	-	-	-	√	√	-	-	-
Solid #1	6:00 bottom of pipe, away from leak	√	√	√	-	√	-	-	-	-	-

Table 2. Results of circumference and diameter measurements performed on the U/S and D/S ends of the pipe sample.

Section End	Circumference (feet)	Diameter Measurements (inches)		
		Diameter from Circumference Measurement	Diameter 3:00 to 9:00	Diameter 6:00 to 12:00
U/S	2.265	8.656	8.625	8.625
D/S	2.270	8.675	8.625	8.625

Table 3. Results of wall thickness measurements performed on the U/S and D/S ends of the pipe sample.

Section End	Wall Thickness <sup>1</sup> (inches)				
	12:00	3:00	6:00	9:00	Average
U/S	0.248	0.248	0.248	0.244	0.247
D/S	0.253	0.249	0.250	0.248	0.250

1 – Measured without coating or significant corrosion.

Table 4. Results of spot tests performed on internal deposits on the pipe sample.

	Solids #1 – Field Test	Deposits on Pipe Surface – Lab Test
Carbonates	Negative	Negative
Sulfides	Negative	Negative
pH	Not performed	8

Table 5. Results of elemental analyses, using EDS, performed on Solid #1; internal deposits removed from the pipe sample.

Element		Solid #1 Average Wt. %
C	(Carbon)	19.0
O	(Oxygen)	29.2
Na	(Sodium)	0.3
Mg	(Magnesium)	0.1
Al	(Aluminum)	0.3
Si	(Silicon)	0.8
S	(Sulfur)	1.1
Cl	(Chlorine)	1.9
K	(Potassium)	2.0
Ca	(Calcium)	0.5
Mn	(Manganese)	0.3
Fe	(Iron)	44.5

Table 6. Composition analysis results for sample Liquid #1.

Cations/Anions	Results	Units	Volatile Fatty Acids (VFAs)	Result	Units
Aluminum	ND	–	Acetate	<1.67	ppm
Barium	0.8	mg/L	Butyrate	<1.67	ppm
Calcium	24.5	mg/L	Formate	<1.67	ppm
Iron	63.4	mg/L	Lactate	<1.67	ppm
Magnesium	7.1	mg/L	Propionate	<1.67	ppm
Manganese	4.5	mg/L	Valerate	<1.67	ppm
Potassium	20,300.0	mg/L			
Silicon	2,420.0	mg/L			
Sodium	135.0	mg/L			
Strontium	0.4	mg/L			
Bromide	ND	mg/L			
Chloride	17,700	mg/L			
Fluoride	91	mg/L			
Sulfate	131	mg/L			
Nitrite	ND	mg/L			
Nitrate	0.78	mg/L			

Table 7. Results of bacteria culture testing performed on Liquid #1 and Swab Samples A, B and C, collected over a ~1 cm<sup>2</sup> area from the internal surface of the pipe sample.

Bacteria Type	Liquid #1		Swab A (Leak)		Swab B (6:00 Away)		Swab C (12:00 Away)	
	Test Result	Number of Positive Vials	Test Result	Number of Positive Vials	Test Result	Number of Positive Vials	Test Result	Number of Positive Vials
Aerobic (AERO)	Positive	1	Positive	4	Positive	4	Positive	5
Anaerobic (ANA)	Positive	1	Not detected	–	Not detected	–	Not detected	–
Acid-Producing (APB)	Positive	1	Positive	2	Not detected	–	Positive	3
Sulfate-Reducing (SRB)	Not detected	–	Not detected	–	Not detected	–	Not detected	–
Iron-Reducing (IRB)	Not detected	–	Not detected	–	Not detected	2	Positive	2
Nitrate-Reducing (NRB)	Positive	1	Positive	2	Positive	2	Positive	3

Table 8. Results of optical microscopy examination of Liquid #1 and Swab Samples A, B and C, collected over a ~1 cm<sup>2</sup> area from the internal surface of the pipe sample.

Sample Identification	Aliquot Volume, uL	Total Cells Observed	Calculated No cells/ cm <sup>2</sup>	Morphology
Liquid #1	10	0	None	-
Swab A (Leak)	10	> 100	>7.00 X 10 <sup>4</sup>	Rods, clusters
Swab B (6:00 Away)	5	> 100	>1.40 X 10 <sup>5</sup>	Rods, clusters
Swab C (12:00 Away)	5	> 100	>1.40 X 10 <sup>5</sup>	Rods, clusters

Table 9. Results of bacteria DNA testing, using quantitative polymerase chain reaction, performed on Liquid #1 and Solid #1 samples.

Target Population / Functional Gene	Abbreviation	Liquid #1 cells/mL	Solid #1 cells/cm <sup>2</sup>
Total Bacteria	EBAC	<b>1.70E+05</b>	<b>1.37E+08</b>
Total Archaea	ARC	< 3.85E+02	1.47E+04 <sup>(J)</sup>
Sulfate reducing bacteria	APS	< 3.85E+02	< 2.38E+04
Sulfate reducing archaea	SRA	< 3.85E+02	< 2.38E+04
Methanogens	MGN	< 3.85E+02	< 2.38E+04
Acetogens	AGN	< 3.85E+02	< 2.38E+04
Fermenters	FER	1.44E+02 <sup>(J)</sup>	< 2.38E+04
Iron reducing bacteria – other	IRB	< 3.85E+02	< 2.38E+04
IRB Geobacter	IRG	< 3.85E+02	< 2.38E+04
IRB Shewanella	IRS	< 3.85E+02	< 2.38E+04
IRB Anaeromyxobacter	IRN	<b>4.26E+03</b>	<b>2.27E+05</b>
Iron Reducing Archaea	IRA	< 3.85E+02	< 2.38E+04
Iron oxidizers	FeOB	< 3.85E+02	<b>4.47E+05</b>
Manganese Oxidizing Bacteria	MnOB	< 3.85E+02	< 2.38E+04
Sulfur oxidizing Bacteria	SOB	1.20E+02 <sup>(J)</sup>	5.41E+03 <sup>(J)</sup>
Denitrifying bacteria	nirK	< 3.85E+02	< 2.38E+04
Denitrifying bacteria	nirS	< 3.85E+02	< 2.38E+04
Ammonia Oxidizing Bacteria	AMO	< 3.85E+02	< 2.38E+04
Nitrite oxidizing bacteria	NOR	< 3.85E+02	< 2.38E+04
Nitrogen Fixers	NIF	< 3.85E+02	<b>3.35E+05</b>
<i>Burkholderia cepacian</i> exopolysaccharide	BCE	< 3.85E+02	< 2.50E+03
<i>Deinococcus</i> spp.	DCS	< 3.85E+02	1.38E+04 <sup>(J)</sup>
<i>Meiothermus</i> spp.	MTS	< 3.85E+02	< 2.38E+04
<i>Cladosporium</i> spp.	CLAD	< 3.85E+02	< 2.38E+04

(J) – Estimated gene copies below PQL (practical quantitation limit)



Table 10. Results of tensile tests performed on transverse base metal and seam weld specimens removed from the pipe sample compared with requirements for API 5LX Grade X42 line pipe steel.

Property	Transverse Base Metal	Transverse Weld Metal	API 5LX Grade X42 Welded Pipe <sup>2</sup>
Yield Strength, ksi <sup>1</sup>	48.1	53.8	42 min
Tensile Strength, ksi <sup>1</sup>	66.2	72.8	60 min
Elongation in 2 inches, %	31.8	22.3	26.0 min
Reduction of Area, % <sup>1</sup>	35.3	24.1	–

1 – Average of duplicate tests.

2 – API 5LX Line Pipe Specifications, 23<sup>th</sup> Edition – March 1981.

Table 11. Results of Charpy V-notch impact tests performed on transverse base metal specimens removed from the pipe sample.

Specimen ID	Temperature (°F)	Sub-Size Impact Energy <sup>1</sup> (ft-lbs)	Full Size Impact Energy <sup>2</sup> (ft-lbs)	Lateral Expansion (mils)	Shear (%)
1	-100	1.0	1.8	0	0
2	-50	0.5	0.9	0	0
3	-25	2.0	3.6	1	0
4	20	4.0	7.2	3	0
5	45	4.0	7.2	2	20
6	60	13.0	23.3	33	70
7	70	16.0	28.7	26	80
8	95	19.0	34.0	39	100
9	150	20.0	35.8	40	100
10	225	20.0	35.8	42	100

1. 0.394 inches × 0.220 inches.

2. Determined from sub-sized specimens. Full size impact energy values were calculated based on the ratio of the cross sectional areas of the specimens at the notch.

Table 12. Results of Charpy V-notch impact tests performed on centerline transverse seam weld specimens removed from the pipe sample.

Specimen ID	Temperature (°F)	Sub-Size Impact Energy <sup>1</sup> (ft-lbs)	Full Size Impact Energy <sup>2</sup> (ft-lbs)	Lateral Expansion (mils)	Shear (%)
1	-150	0.5	1.0	0	0
2	-100	1.0	2.0	0	0
3	-30	4.0	8.1	2	0
4	-5	6.5	13.1	7	5
5	20	8.0	16.2	13	20
6	45	9.0	18.2	4	50
7	70	11.0	22.2	18	60
8	95	15.0	30.3	22	100
9	150	11.5	23.2	25	100
10	225	12.0	24.2	30	100

- 0.394 inches × 0.195 inches.
- Determined from sub-sized specimens. Full size impact energy values were calculated based on the ratio of the cross sectional areas of the specimens at the notch.

Table 13. Results of analyses of the Charpy V-notch impact energy and percent shear plots for transverse base metal and seam weld metal specimens removed from the pipe sample.

	Base Metal	Seam Weld
Upper Shelf Impact Energy (Full Size), Ft-lbs	35.2	24.0
85% FATT, °F	69	97
85% FATT, °F (Full Size) <sup>1</sup>	58	94

- Full Scale Pipe FATT = 85%FATT +  $((66 * (t_w^{0.55} / t_c^{0.7}) - 100)$  where  $t_w$  = pipe wall thickness and  $t_c$  = width of the CVN specimen.

Table 14. Results of elemental analysis, using optical emission spectroscopy, performed on a base metal sample removed from the pipe sample.

Element		Base Metal	API 5LX Grade X42 Welded Pipe <sup>1</sup>
C	(Carbon)	0.216	0.28 max
Mn	(Manganese)	1.101	1.25 max
P	(Phosphorus)	0.04	0.045 max
S	(Sulfur)	0.05	0.06 max
Si	(Silicon)	0.014	Not specified
Cu	(Copper)	0.066	Not specified
Sn	(Tin)	0.002	Not specified
Ni	(Nickel)	0.019	Not specified
Cr	(Chromium)	0.018	Not specified
Mo	(Molybdenum)	0.005	Not specified
Al	(Aluminum)	0.001	Not specified
V	(Vanadium)	0.000	Not specified
Nb	(Niobium)	0.001	Not specified
Zr	(Zirconium)	0.001	Not specified
Ti	(Titanium)	0.001	Not specified
B	(Boron)	0.000	Not specified
Ca	(Calcium)	0.000	Not specified
Co	(Cobalt)	0.016	Not specified
Fe	(Iron)	Balance	Balance

1 – API 5LX Line Pipe Specifications, 23<sup>th</sup> Edition – March 1981.

Table 15. Five-Year Averages for Carbon Dioxide, Nitrogen, and Water Vapor at Four Aliso Canyon Gas Monitoring Locations.

Gas Component	Gas Monitoring Location			
	Dehy 1 (inlet)	Dehy 2 (Inlet)	KVS	TDC
CO <sub>2</sub> , mol%	0.89	0.94	1.08	1.03
N <sub>2</sub> , mol%	0.36	0.41	0.36	0.34
H <sub>2</sub> O, lbs/Mscf	7.74	28.23	–	–



Figure 1. View of the well line looking west (downstream). Approximate axial location of the leak is indicated by the arrow. The pipeline is relatively horizontal here and the leak was at a slight sag or low spot.



Figure 2. View from a location just upstream of the leak, looking east (upstream). Well location is beyond the top of the hill



Figure 3. Surface swabs, solid, and liquid samples collected by DNV GL personnel in the field when the pipe section was cut out.



Figure 4. Photograph showing the as-received condition of the pipe sample; wrapped in plastic with the ends sealed.

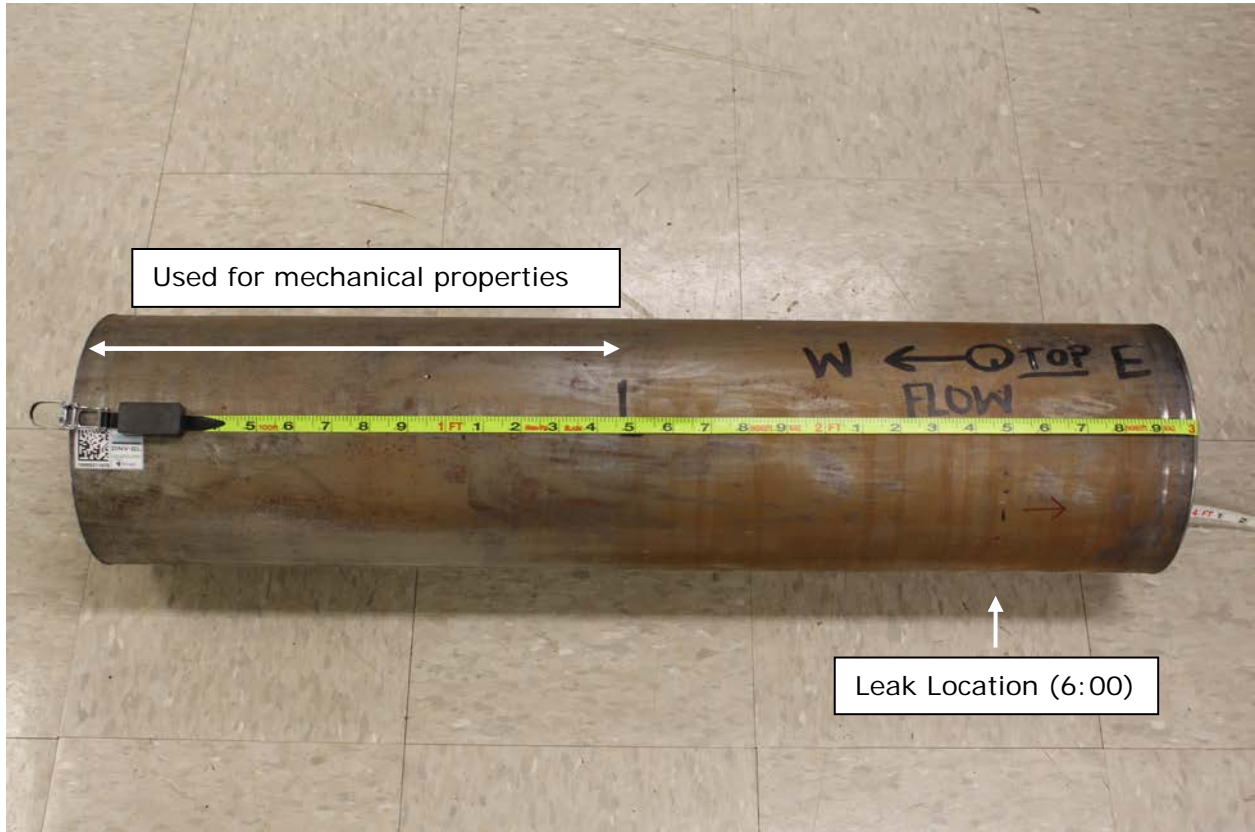


Figure 5. Photograph showing the pipe sample after unwrapping at the DNV GL lab. Flow direction and 12:00 position are marked on the pipe. Approximately half of the sample was used to machine specimens for mechanical testing. Location of leak (at 6:00) shown at arrow.



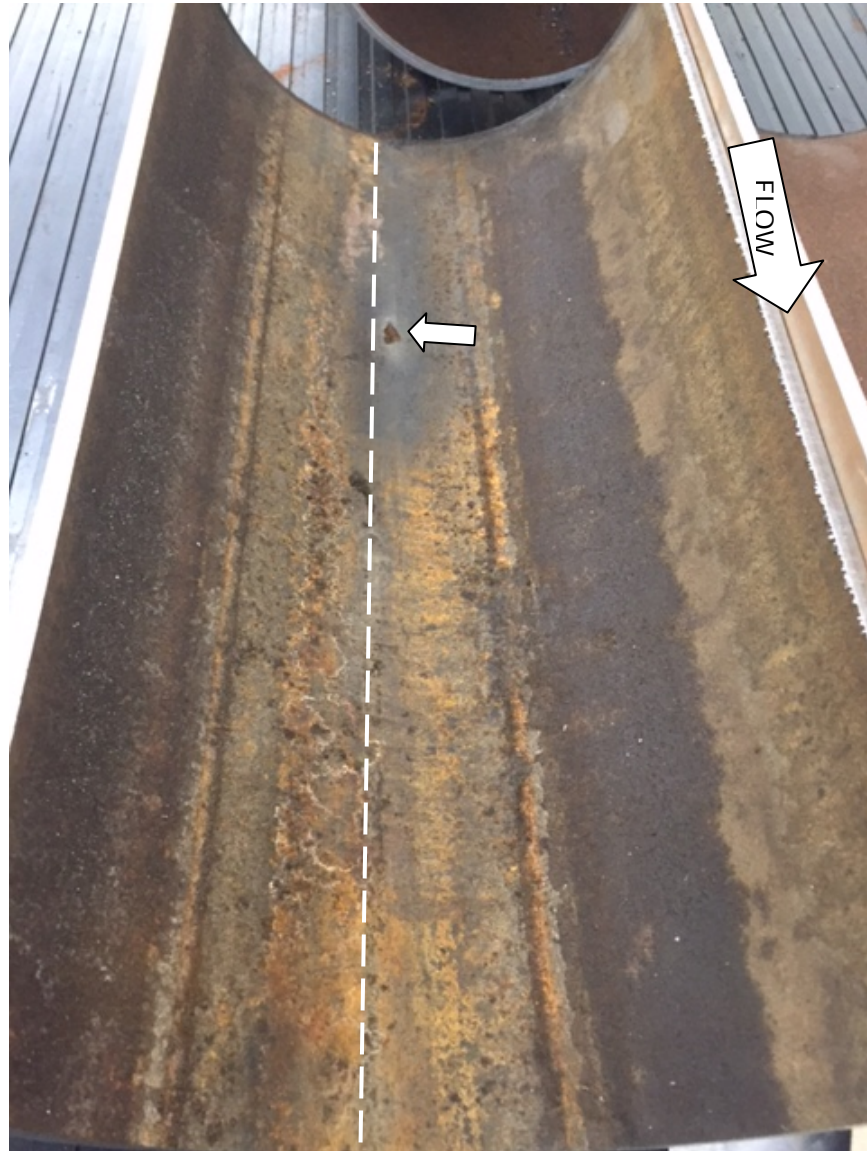


Figure 6. Photograph showing a portion of the bottom half of the internal surface of pipe sample after it was split by cutting at the 3 and 9 orientations. The 6:00 orientation is shown by the dashed line and the leak/pit is shown at the arrow. Coloration of deposits on the internal surface illustrates historical liquid-level lines.

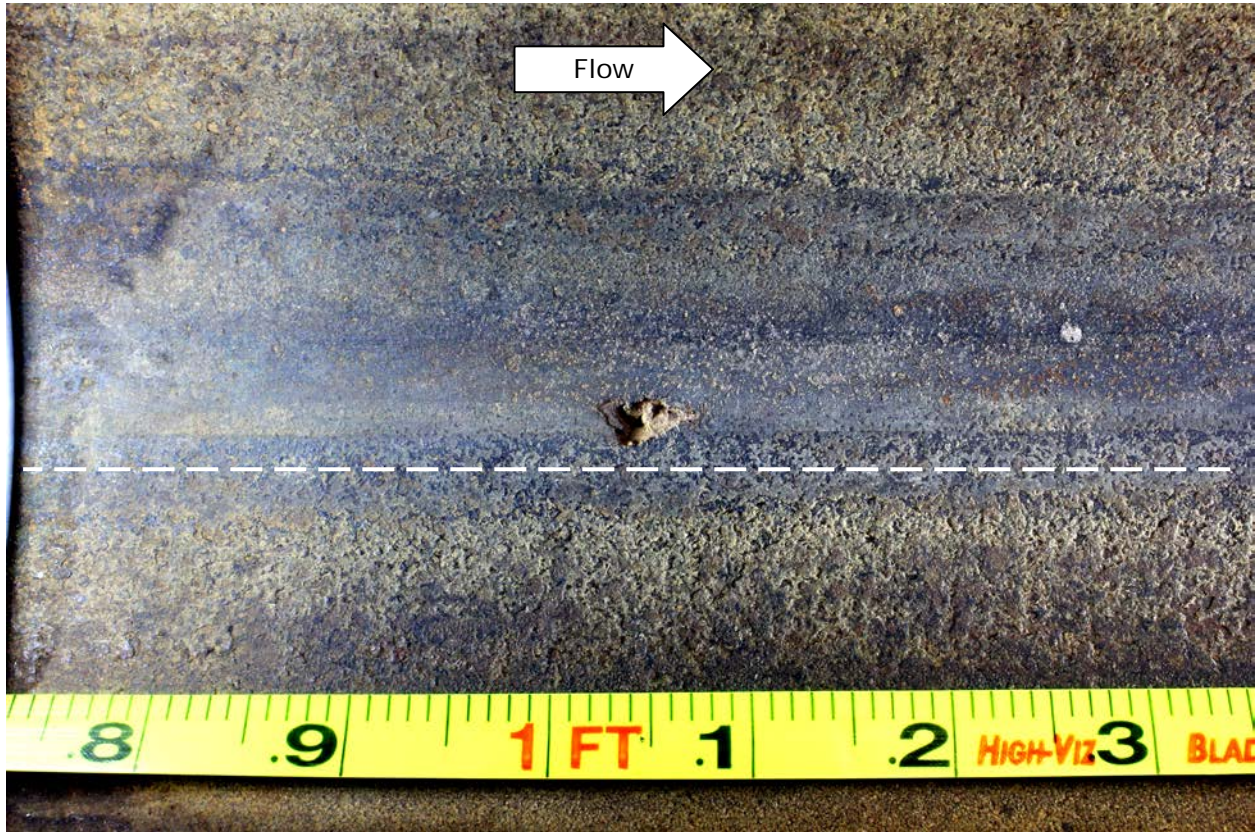


Figure 7. Photograph showing the internal pipe surface at the leak/pit location after cleaning, dashed line shows the 6:00 orientation.



Figure 8. Photograph of the internal pipe surface at the leak/pit after cleaning.

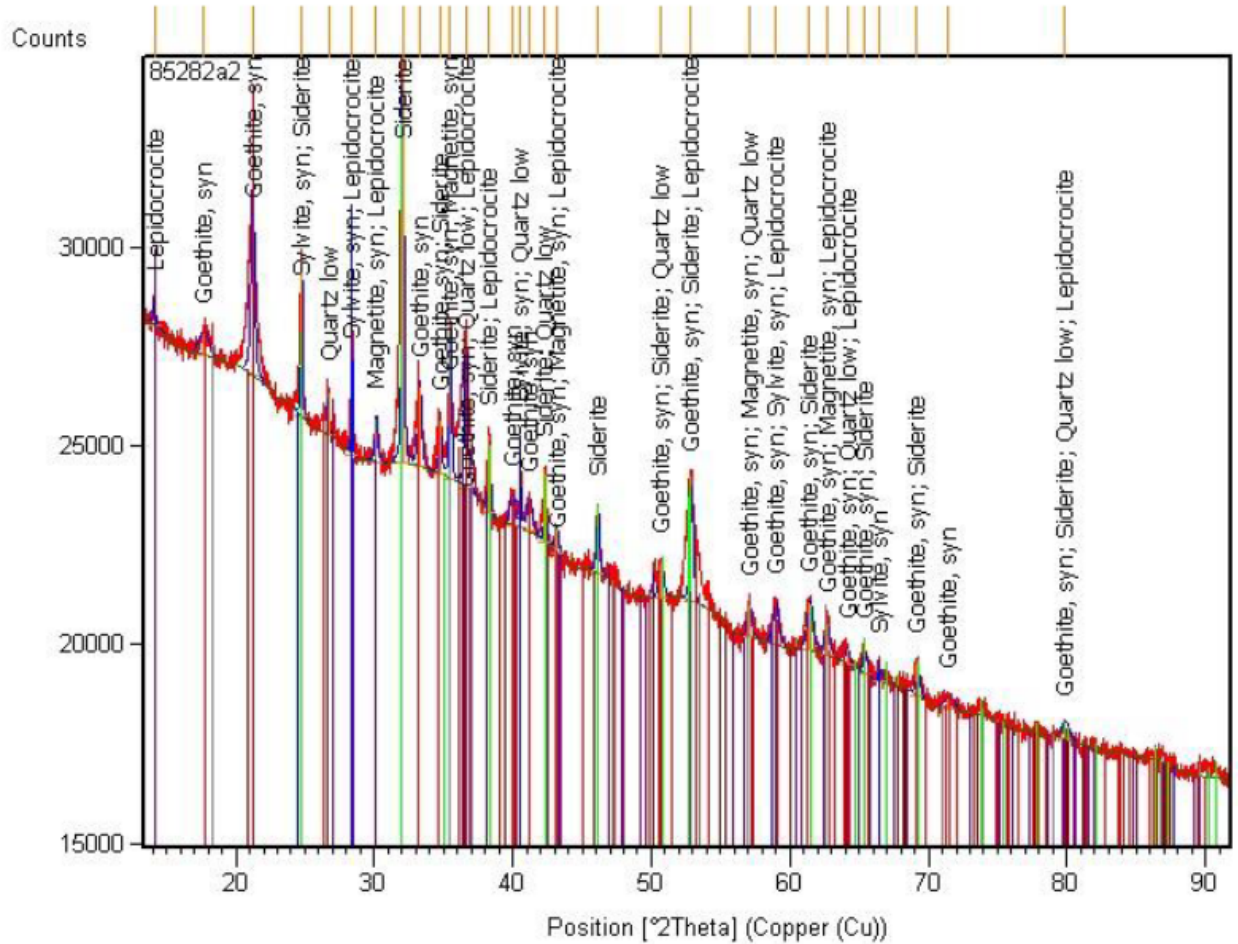


Figure 9. XRD powder diffraction pattern of sample Solid #1.

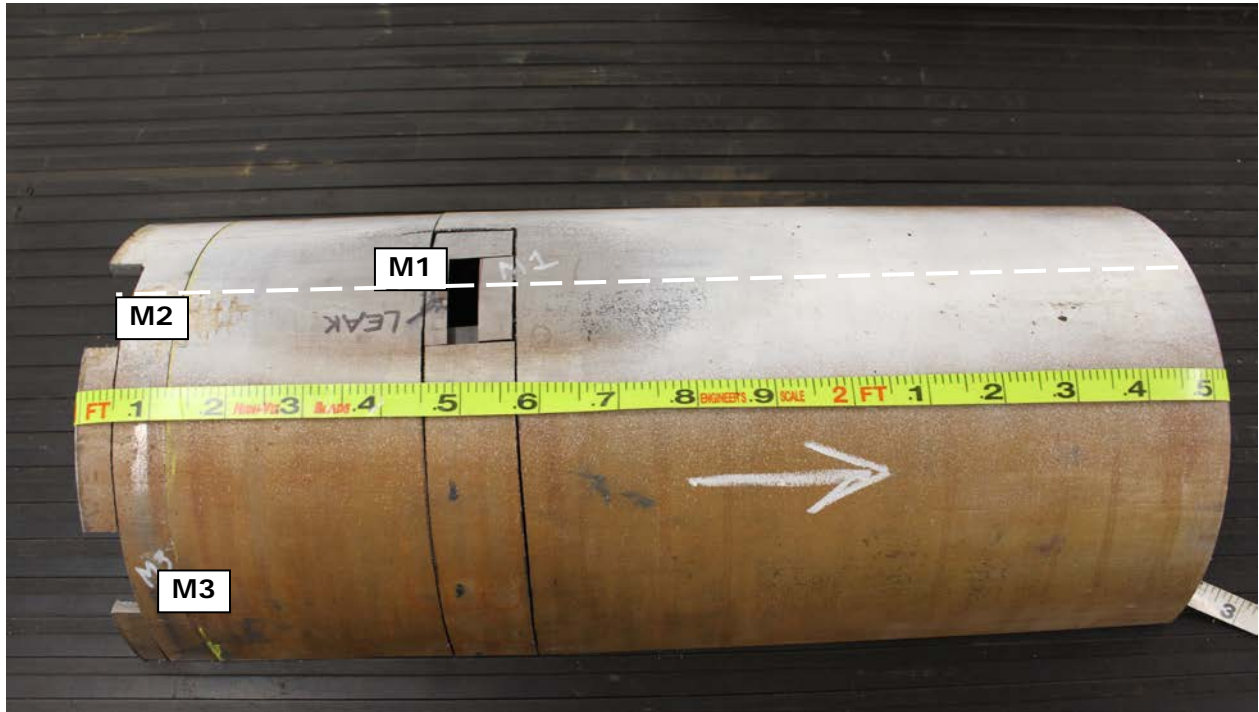


Figure 10. Photograph showing the locations of three specimens removed for preparation of metallographic mounts from the pipe sample; M1 from the leak location, M2 from the ERW longitudinal seam and M3 from the pipe body. Dashed line shows orientation of ERM seam.

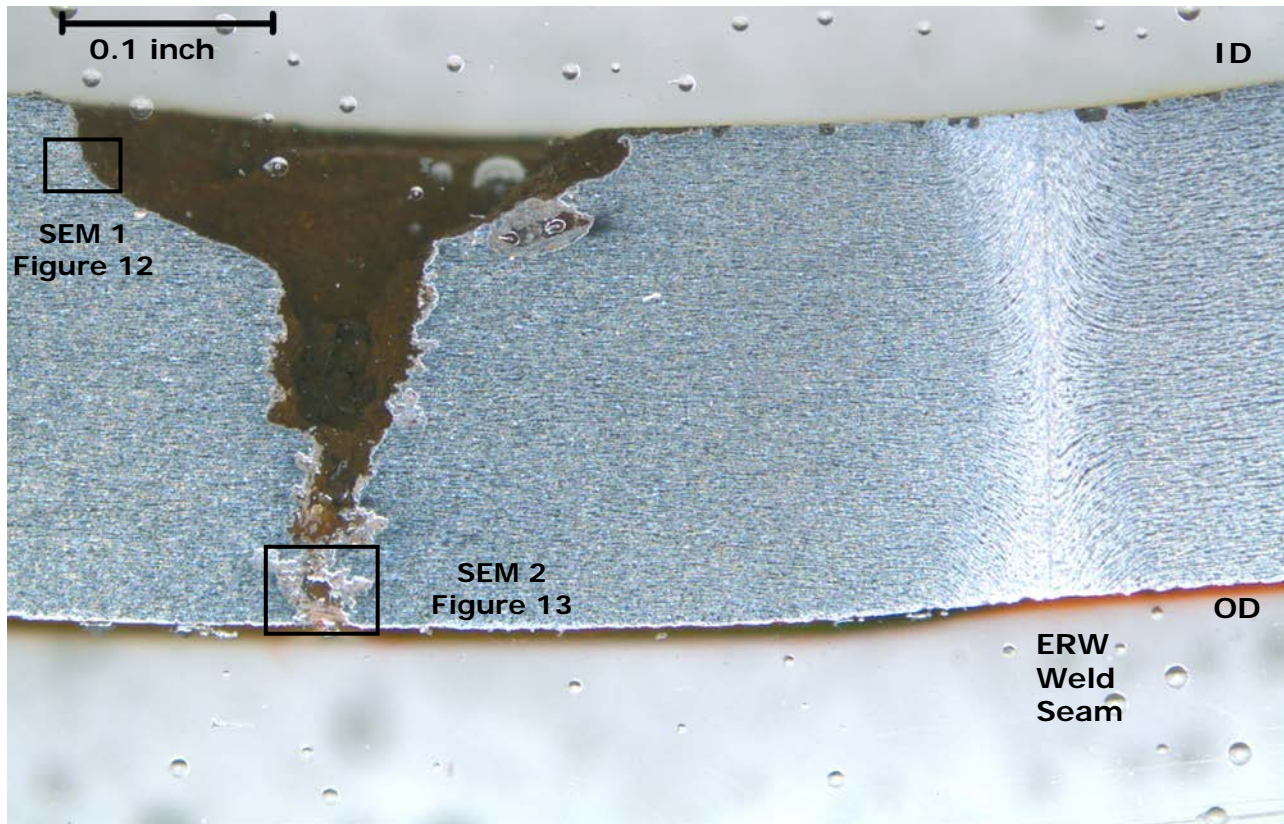


Figure 11. Photomicrograph of Mount M1, showing the pit/leak (left) and the ERW weld seam (right). Areas that were analyzed using SEM/EDS are shown by the boxes labelled SEM 1 and SEM 2. Nital etch.

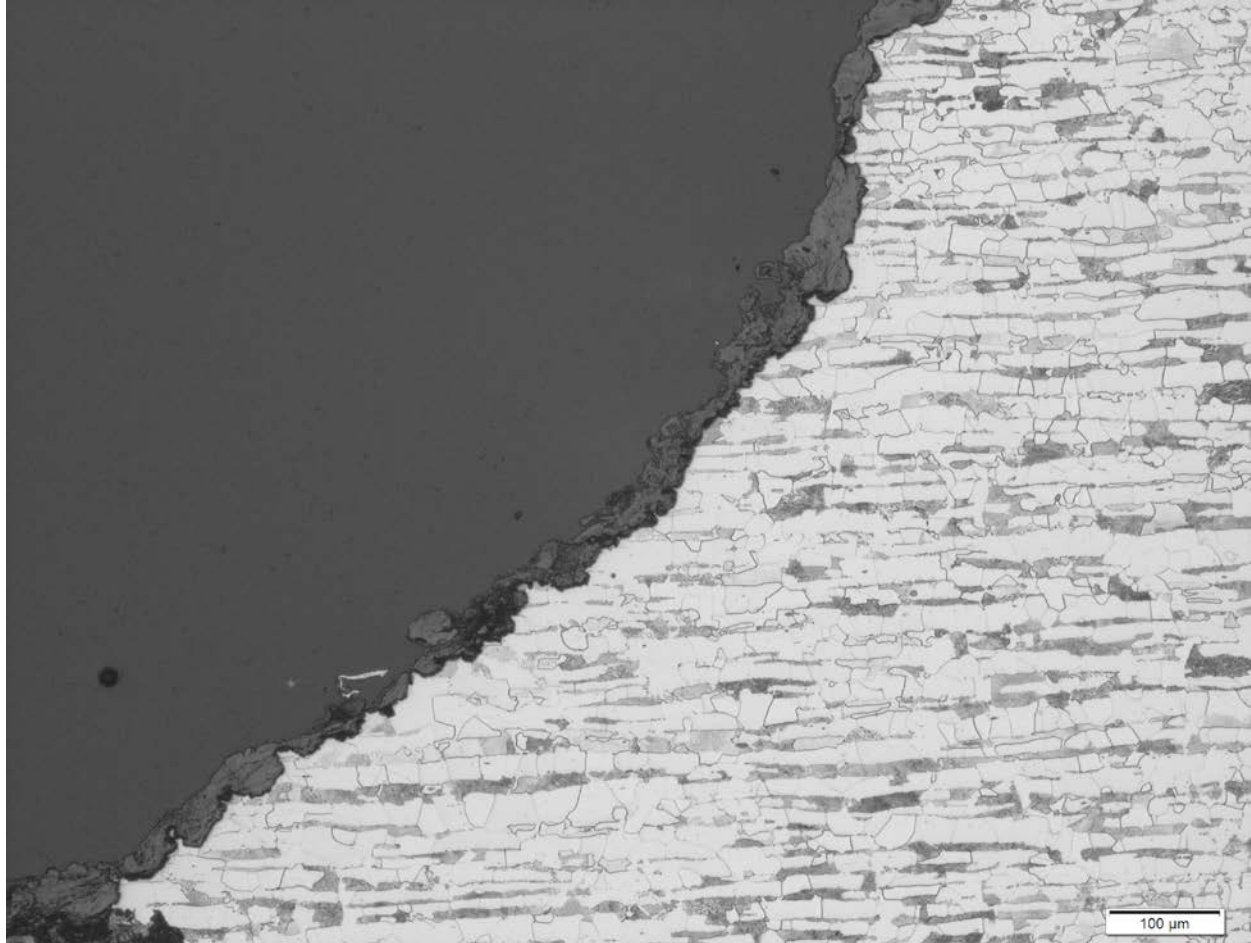


Figure 12. Photomicrograph of Mount M1 along the edge of the smooth, parabolic shaped zone of the pit cross section nearest the internal surface of the pipe. Magnification – 100X. Nital etch. (ID surface towards the top of photo; mirror image or area shown in Figure 11).

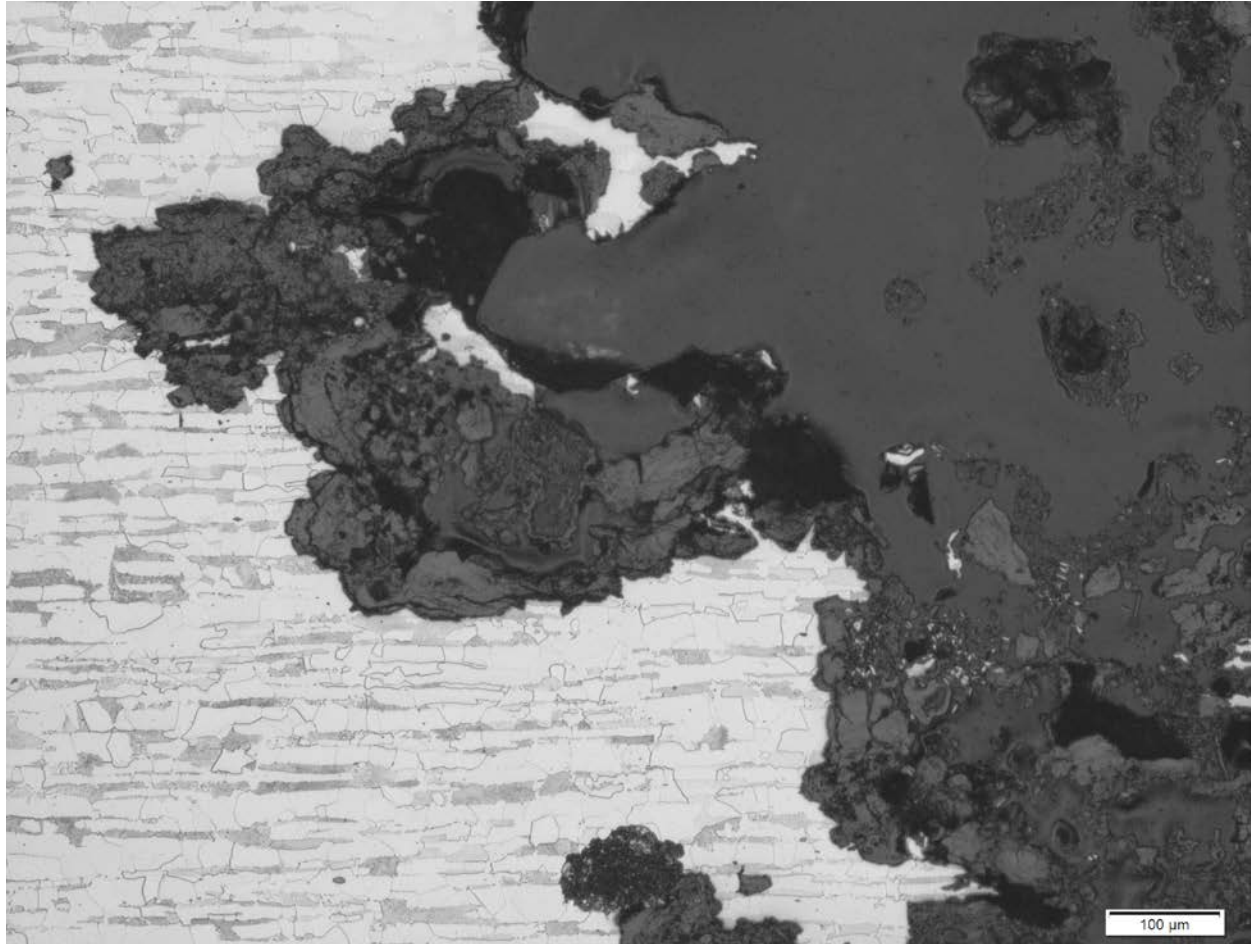


Figure 13. Photomicrograph of Mount M1 along the edge of the narrow zone in the pit cross section showing significant undercutting. Magnification – 100X. Nital etch. (ID surface towards the top of photo; mirror image or area shown in Figure 11).



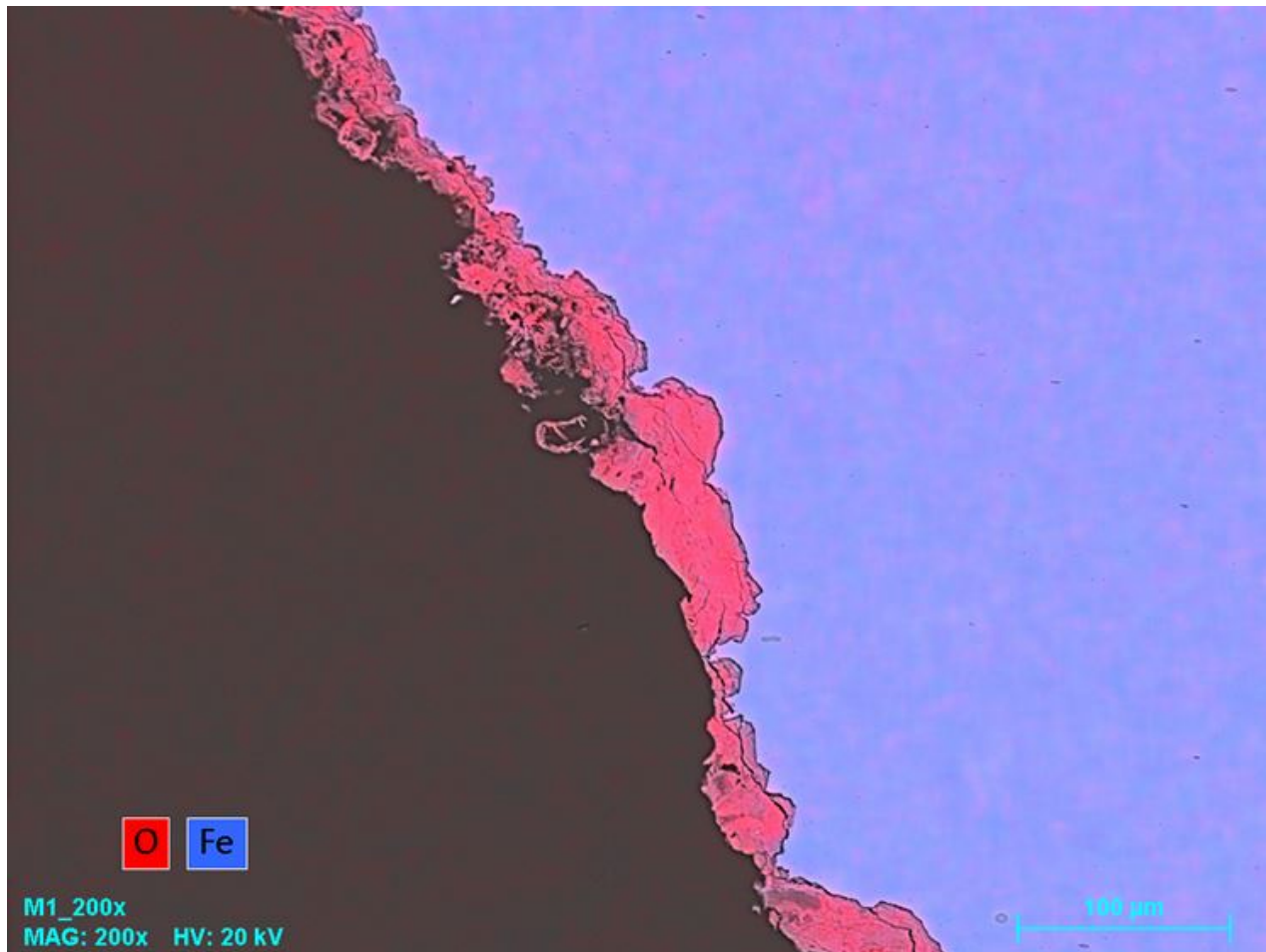


Figure 14. SEM/EDS composite image showing distribution of iron (Fe) and oxygen (O) in the deposit layer on the pit surface in the smooth, parabolic zone, location SEM 1 in Figure 11. Original magnification – 200X.

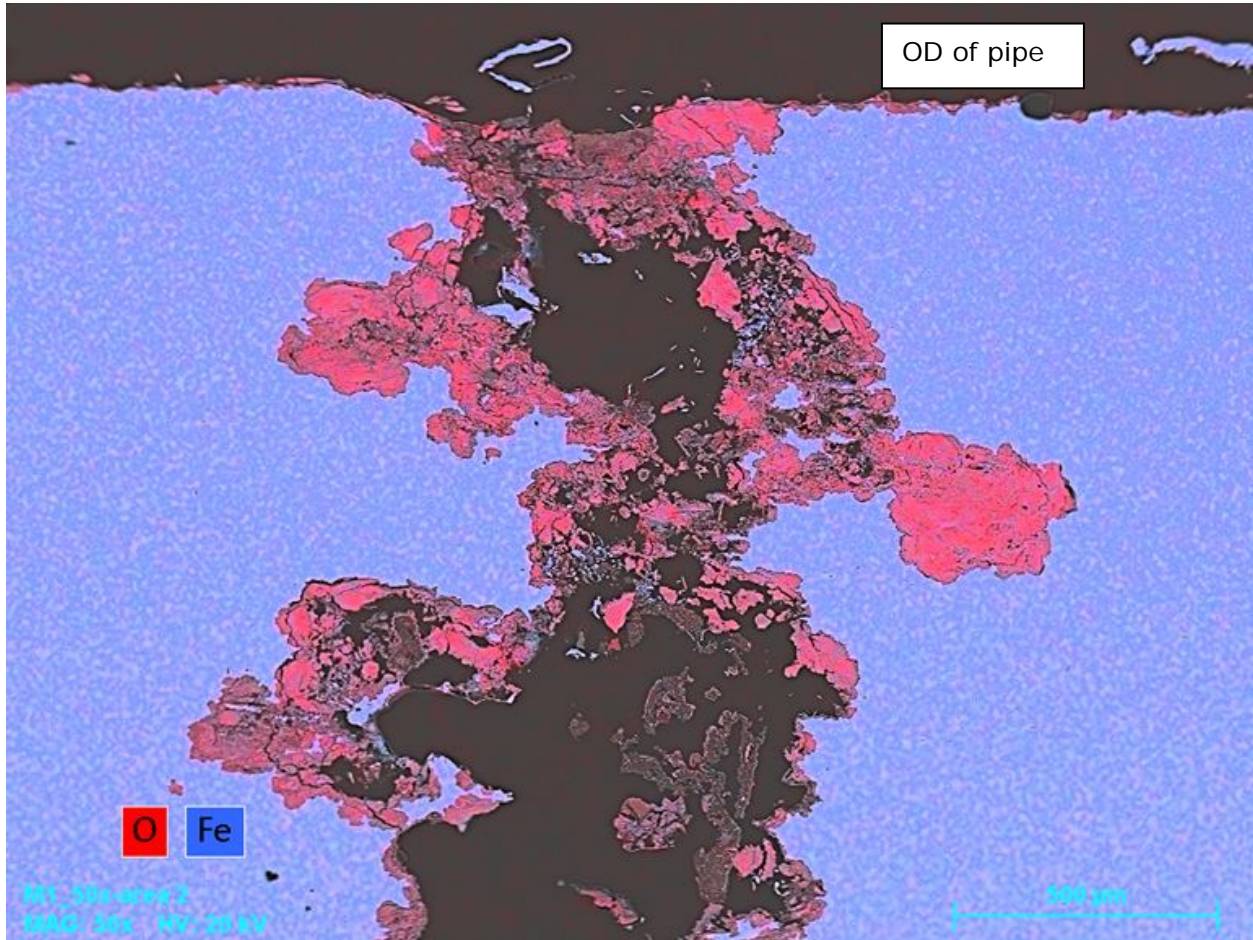


Figure 15. SEM/EDS composite image showing distribution of iron (Fe) and oxygen (O) in the scale layer on the pit surface near the leak at the OD surface, location SEM 2 in Figure 11; original magnification – 50X. (Image inverted from its actual position in service.)

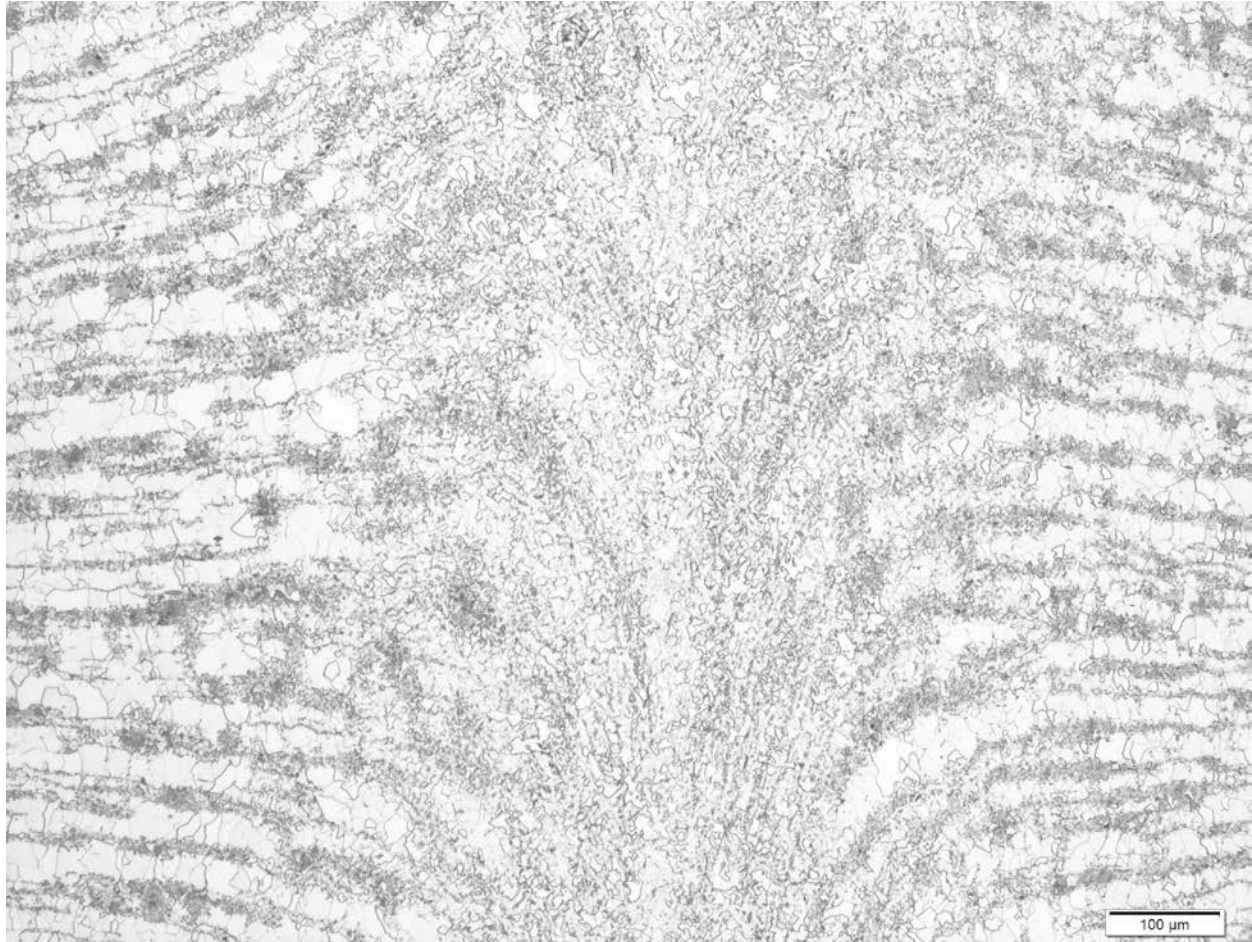


Figure 16. Photomicrograph of Mount M2 showing the centerline of the ERW seam weld (center of photo). Magnification – 100X. Nital etch.



Figure 17. Photomicrograph of Mount M3 showing the microstructure of the pipe body away from the leak and away from the ERW weld. Magnification – 100X. Nital etch.

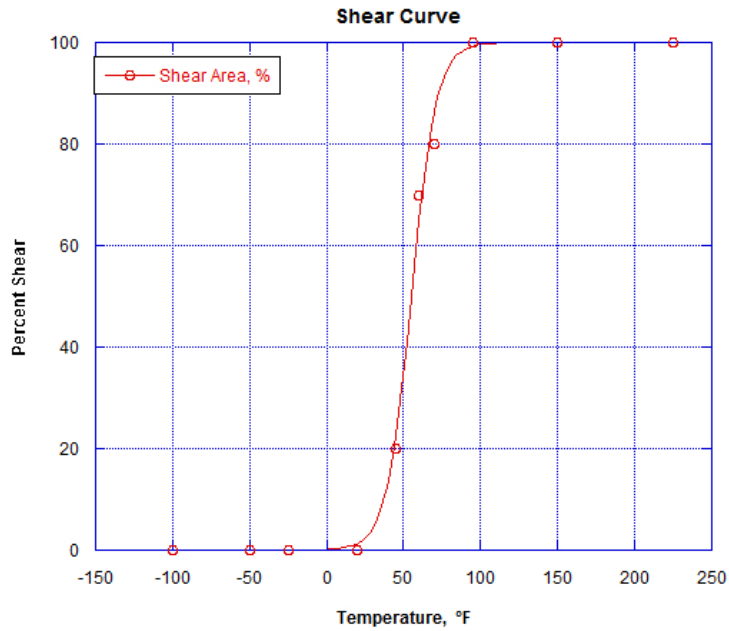


Figure 18. Percent shear from Charpy V-notch tests as a function of temperature for transverse specimens removed from the base metal of the pipe sample.

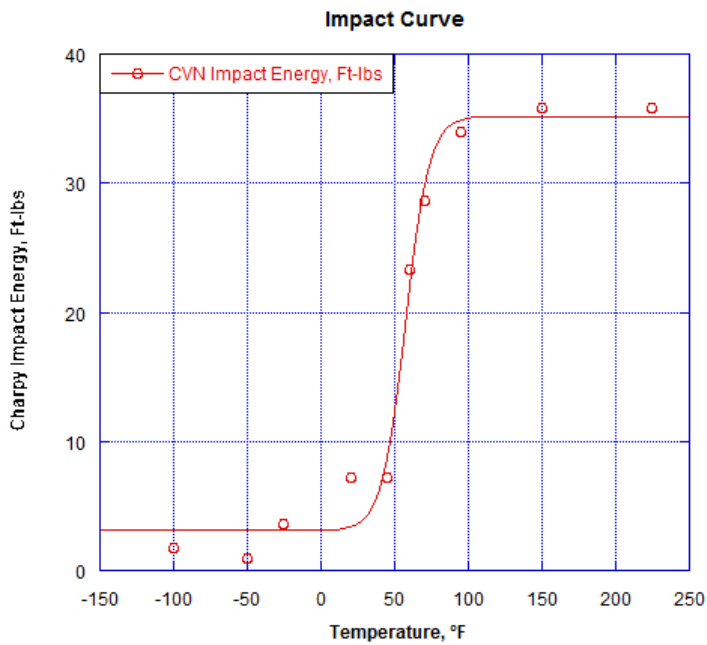


Figure 19. Charpy V-notch impact energy as a function of temperature for transverse specimens removed from the base metal of the pipe sample.

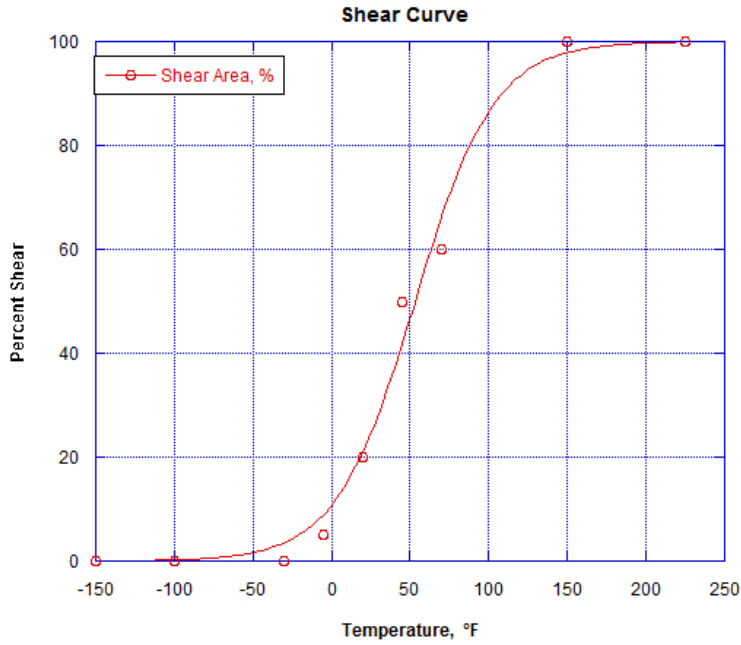


Figure 20. Percent shear from CVN tests as a function of temperature for transverse specimens removed from the seam weld centerline of the pipe sample.

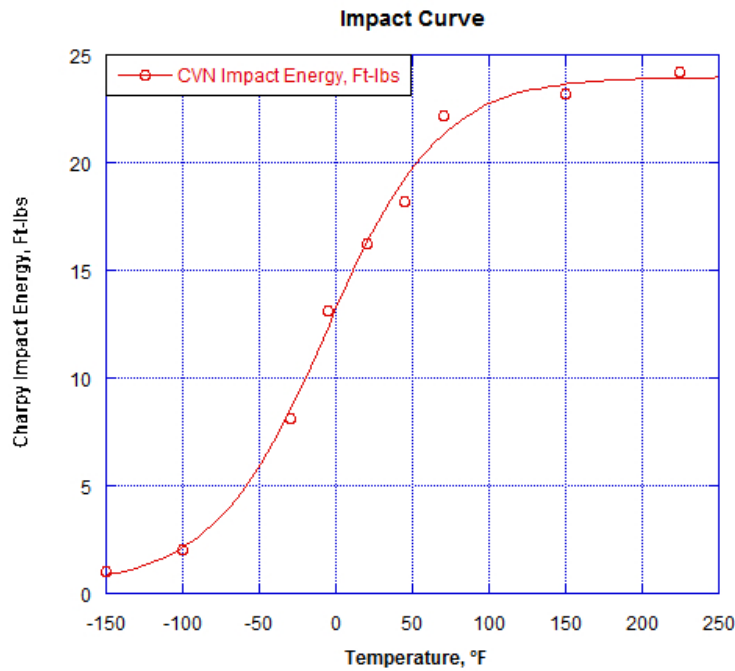
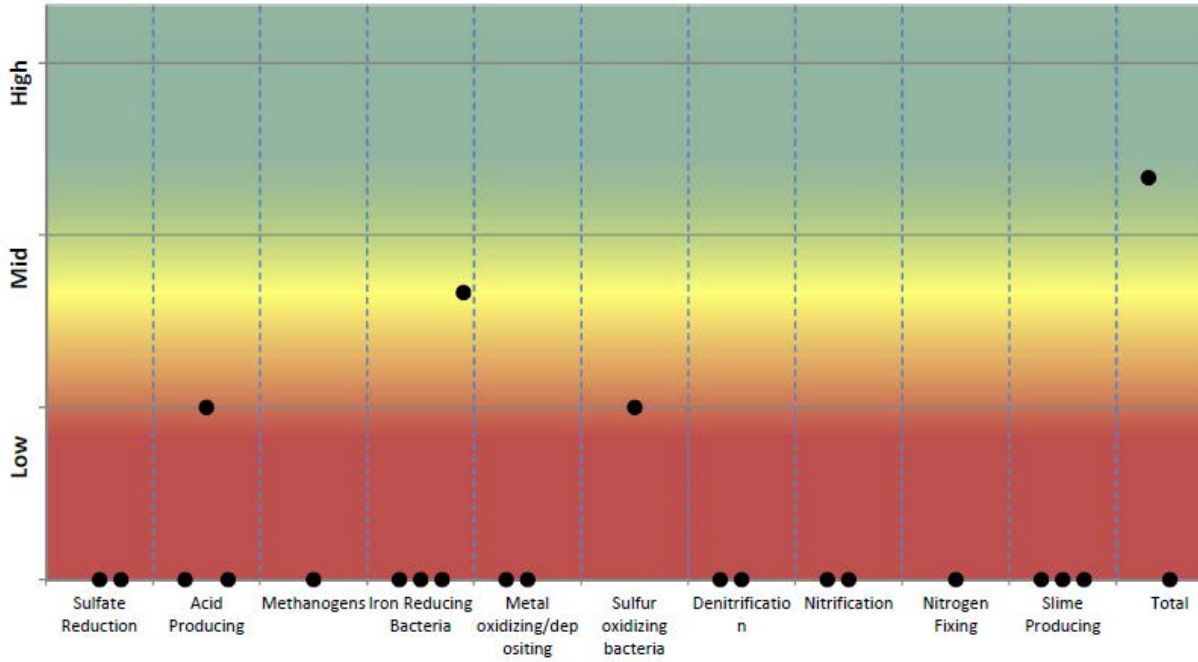


Figure 21. CVN impact energy as a function of temperature for transverse specimens removed from the seam weld of the pipe sample.

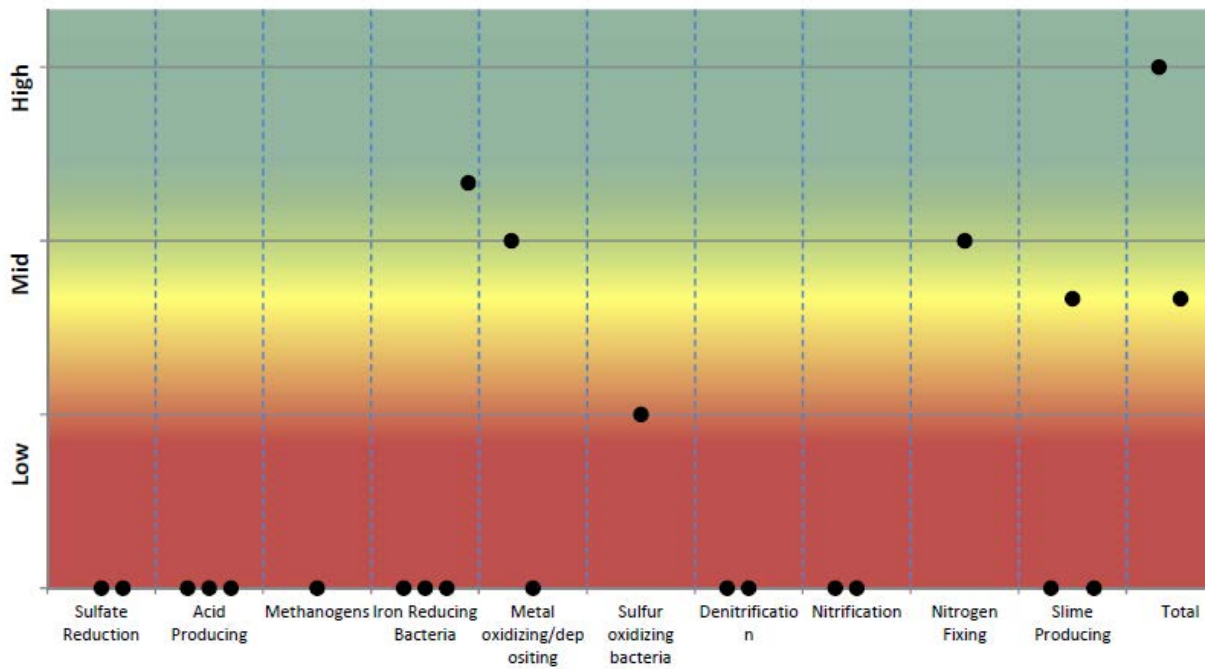
## **APPENDIX A**

### **Summary of qPCR Results Liquid #1 and Solid #1 Samples**

**Liquid #1 Sample – Summary of microbiological populations.**



**Solid#1 Sample – Summary of microbiological populations.**







## **ABOUT DNV GL**

Driven by our purpose of safeguarding life, property, and the environment, DNV GL enables organizations to advance the safety and sustainability of their business. We provide classification and technical assurance along with software and independent expert advisory services to the maritime, oil and gas, and energy industries. We also provide certification services to customers across a wide range of industries. Operating in more than 100 countries, our 16,000 professionals are dedicated to helping our customers make the world safer, smarter, and greener.